SPECIAL REPORT 99-14

US Army Corps of Engineers®
Cold Regions Research & Engineering Laboratory

Resilient Modulus for New Hampshire Subgrade Soils for Use in Mechanistic AASHTO Design

Vincent C. Janoo, John J. Bayer Jr., Glenn D. Durell, and Charles E. Smith Jr.

September 1999

Abstract: Resilient modulus tests were conducted on five subgrade soils commonly found in the state of New Hampshire. Tests were conducted on samples prepared at optimum density and moisture content. To determine the effective resilient modulus of the various soils for design purposes, tests were conducted at room temperature and at freezing temperatures. The AASHTO TP 46 test protocol was used for testing room temperature and thawing soils. At freezing temperatures, the CRREL test protocol was used. The results from this test program are presented in this report. In addition, suggested effective resilient modulus for the five soils are presented.

How to get copies of CRREL technical publications:

Department of Defense personnel and contractors may order reports through the Defense Technical Information Center:

DTIC-BR SUITE 0944
8725 JOHN J KINGMAN RD
FT BELVOIR VA 22060-6218
Telephone 1 800 225 3842
E-mail help@dtic.mil
msorders@dtic.mil
WWW http://www.dtic.dla.mil/

All others may order reports through the National Technical Information Service:

NTIS
5285 PORT ROYAL RD
SPRINGFIELD VA 22161
Telephone 1 800 553 6847 or 1 703 605 6000
1 703 487 4639 (TDD for the hearing-impaired)
E-mail orders@ntis.fedworld.gov
WWW http://www.ntis.gov/index.html

A complete list of all CRREL technical publications is available from:

USACRREL (CEERD-IM-HL)
72 LYME RD
HANOVER NH 03755-1290
Telephone 1 603 646 4338
E-mail techpubs@crrel.usace.army.mil

For information on all aspects of the Cold Regions Research and Engineering Laboratory, visit our World Wide Web site: http://www.crrel.usace.army.mil

Special Report 99-14

US Army Corps of Engineers®
Cold Regions Research & Engineering Laboratory

Resilient Modulus for New Hampshire Subgrade Soils for Use in Mechanistic AASHTO Design

Vincent C. Janoo, John J. Bayer Jr., Glenn D. Durell, and Charles E. Smith Jr.

September 1999

Prepared for
OFFICE OF THE CHIEF OF ENGINEERS

PREFACE

This report was prepared by Dr. Vincent C. Janoo, Research Civil Engineer, and John J. Bayer Jr., Glenn D. Durell, and Charles E. Smith Jr., Engineering Technicians, of the Civil Engineering Research Division, U.S. Army Cold Regions Research and Engineering Laboratory (CRREL), Hanover, New Hampshire.

This work was funded through an Intergovernmental Cooperative Agreement (ICA) between the State of New Hampshire, Department of Transportation (NHDOT), and CRREL. This work has been designated as NHDOT Statewide Project 12323P.

The authors thank Glenn Roberts, NHDOT, and Sally Shoop, CRREL, for technically reviewing the manuscript of this report. Thomas Clearly and Paul Matthews of NHDOT and David Hall of FHWA contributed significantly to this review. The authors also thank Lynette Barna for assisting in organizing the report, and Edmund Wright and John Severance for editing and getting the report in its final form. Last but not least, special thanks are due to Dawn Boden and Jane Mason for the illustrations.

This report was prepared in cooperation with the New Hampshire Department of Transportation and the U.S. Department of Transportation, Federal Highway Administration.

CONTENTS

ILLUSTRATIONS

Figure

TABLES

Table

Table

EXECUTIVE SUMMARY

Resilient modulus tests were conducted on five subgrade soils considered to be representative of the subgrade soils found in the state of New Hampshire. Tests were conducted at the optimum density and moisture content. The optimum density and moisture content for the five soils were provided by the New Hampshire Department of Transportation (NHDOT). Although the focus was on resilient modulus tests, a limited number of hydrostatic and triaxial compression tests were conducted.

The tests were conducted to determine the effective resilient modulus of the soils for use in the AASHTO design procedure. Resilient modulus tests were conducted at several temperatures to reflect freezing and thawing. Temperature was selected as the primary variable because it is the easiest to measure in the field. The tests were conducted using the AASHTO TP 46 test protocol, except when the samples were frozen. When frozen, the CRREL testing protocols was used. Although tests were done at different confining pressures and deviator stress, the average values were used to determine the effective modulus. This is justifiable, as the AASHTO design method requires a single resilient modulus value. These values can be used with most mechanistic design methods as they use linear elastic properties. However, the nonlinear information is available in this report for future nonlinear analysis. A limited number of radial strain measurements were made, and Poisson's ratio was calculated. Many of these values were outside the conventional range of Poisson's ratio for elastic materials. This is to be expected since subgrade soils are not linear homogenous material but a conglomeration of aggregates or particles.

Samples were prepared using a kneading compactor. A series of tests were conducted to determine the correct kneading pressure and the number of tamps to provide a uniform density (as a function of depth) for the sample at the optimum moisture content.

The computer program FROST was used to determine the temperature at top of the subgrade for typical interstate and rural pavements. Temperatures for both the Concord and Lebanon, New Hampshire, areas were used in the analysis. It was found that the subgrade temperatures were similar at Concord and Lebanon. The results presented here are for Concord but can be used in most of the state. The exception may be in high areas at higher elevations. The monthly resilient modulus selected was based on the subgrade temperatures, not on the mean air temperatures. The effective resilient modulus for the five soils for each month of the year are presented in the recommendation/conclusion sections. The results presented in this report are for optimum density moisture conditions. Care must be taken with its use at other densities or moisture conditions.

Resilient Modulus for New Hampshire Subgrade Soils for Use in Mechanistic AASHTO Design

VINCENT C. JANOO, JOHN J. BAYER JR., GLENN D. DURELL, AND CHARLES E. SMITH JR.

INTRODUCTION

The American Association of State Highway and Transportation Officials (AASHTO) pavement design procedure is an empirical design method based on the results from the AASHO road tests. The AASHO (the precursor of AASHTO) road tests were conducted near Ottawa, Illinois, around 1958 to 1960. The road tests were conducted on asphalt concrete pavements, portland cement concrete pavements, and bridge decks. A total of 10 lanes were tested under controlled loading ranging from 9-kN (2,000-lbf) single axle loads to 215-kN (48,000-lbf) tandem axle loads. A total of 1,114,000 axle loads were applied during the road test.

The design is based on the functional properties of the pavement structure, such as cracking, rutting, and roughness. This change in the functional properties is indexed by the *present serviceability index* (PSI). The PSI ranges from 0 to 5, with 5 designating excellent conditions. On highway pavement, when the PSI has reached 2.5, major rehabilitation is required. The original design, eq 1, is a relationship between 80-kN (18-kip) axle loads to thickness of the pavement layers and the subgrade at the AASHO road tests:

$$\log W_{t18} = 9.36 \log(SN+1) - 0.20 + \frac{\log\left[(4.2-p_t)/(4.2-1.5)\right]}{0.40+\left[1094/(SN+1)^{5.19}\right]} \quad (1)$$

where W_{t18} = 80-kN total load application at end of time t,

SN = structural number of pavement,

p_t = terminal serviceability index.

Later, eq 1 was modified to account for subgrade soil types other than the type A-6 found at the AASHO Test Road. A soil support term (S_i) was added to eq 1 and is shown in eq 2:

$$\log W_{t18} = 9.36 \log(SN+1) - 0.20 + \frac{\log\left[(4.2-p_t)/(4.2-1.5)\right]}{0.40+\left[1094/(SN+1)^{5.19}\right]} + \log\frac{1}{R} + 0.372(S_i - 3.0) \; . \quad (2)$$

S_i for the AASHO subgrade soil was set at 3.0, and S_i can range between 3 and 10, with 10 representing a crushed rock type subgrade. R is a regional factor introduced to account for climates other than Ottawa, Illinois.

With the introduction of the AASHTO 1996 design guide (AASHTO 1996a), the soil support value was replaced by the effective resilient modulus M_r of the subgrade soil:

$$\log W_{t18} = 9.36 \log(SN+1) - 0.20 + \frac{\log\left[(4.2-p_t)/(4.2-1.5)\right]}{0.40+\left[1094/(SN+1)^{5.19}\right]} + 2.32 \log M_r - 8.07 \; . \quad (3)$$

Equation 3 becomes eq 1 if a resilient modulus equal to 21 MPa (3,000 psi) is estimated for the A-6 subgrade soil at the AASHO road test.

The effective resilient modulus is a single value that produces the same amount of annual damage to the pavement structure when compared with the damage obtained from the use of seasonal subgrade moduli. The relative damage (u_f) (AASHTO 1996a) is calculated from

$$u_f = 1.18 \times 10^8 M_r^{-2.32} . \quad (4)$$

An example for estimating the effective resilient modulus is shown in Figure 1.

The New Hampshire Department of Transportation (NHDOT) is developing effective resilient moduli values for typical subgrade soils found in the state for use in the AASHTO design guide. The soils selected for this project reflected most, but not all, of the subgrade soils found in the state. Resilient modulus tests were conducted on these soils at optimum density and as a function of temperature and moisture content. In addition, some tests were conducted to determine the shear strength properties of the soils. The shear strength may be more critical for predicting damage than the resilient modulus during the spring thaw period.

This report provides the results from the exten-

Month	Roadbed Soil Modulus (psi) M_R	Relative Damage u_f
Jan	20,000	0.01
Feb	20,000	0.01
Mar	2,500	1.51
Apr	4,000	0.51
May	4,000	0.51
Jun	7,000	0.13
Jul	7,000	0.13
Aug	7,000	0.13
Sep	7,000	0.13
Oct	7,000	0.13
Nov	4,000	0.51
Dec	20,000	0.01
Summation: Σu_f		3.72

Average: $\bar{u}_f = \frac{\Sigma u_f}{n} = \frac{3.72}{12} = 0.31$

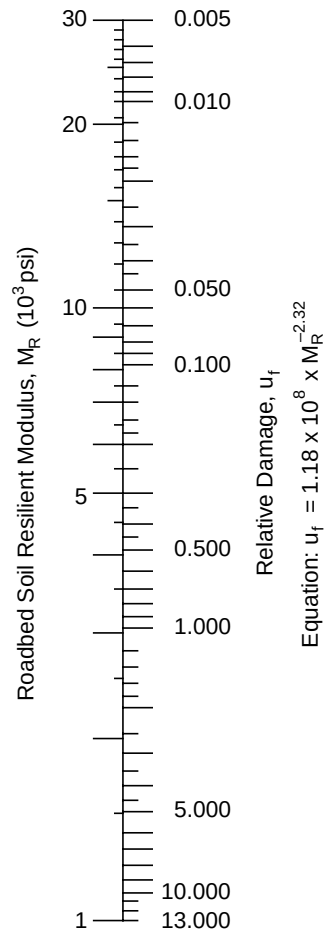

Effective Roadbed Soil Resilient Modulus, M_R (psi) = 5,000 (Corresponds to $\bar{u}_f$)

Figure 1. Chart for estimating effective roadbed soil resilient modulus for flexible pavement designed using the serviceability criteria (after AASHTO 1996).

sive laboratory testing to determine the resilient modulus of the various subgrade soils as a function of temperature. It also provides a guide for selecting the appropriate resilient modulus values to be used in the current AASHTO design method. These values can also be used in future modifications to the AASHTO design method as proposed in the current AASHTO 2002 design guide research study.

DESCRIPTION OF TEST SOILS

The five test soils selected for this project, after discussion with NHDOT personnel, reflected most, but not all, of the subgrade soils in New Hampshire. With the exception of the marine clay, the grain size gradation and moisture density relationships were provided by the NHDOT. The grain size gradation, Atterberg's limits, and moisture density relationship for the marine clay were conducted at CRREL. The gradations are shown in Figure 2. The classification and optimum moisture density are shown in Table 1. All moisture density relationships were developed using the AASHTO T99A Proctor Test Specifications. The liquid limit (LL) and plasticity index (PI) for the marine clay were 50 and 17%, respectively.

TEST PROGRAM

In accordance to AASHTO TP46-94 (1996b), the coarse gravelly sand (A-1-a) and the silty glacial till (A-4) were compacted into 152-mm- (6-in.-) diam. × 30-mm- (12-in.-) high samples, These soils are designated as base / subbase materials according to AASHTO TP46-94. The remaining sand (A-1-b) and fine-grained soils (A-2-4 and A-7-5) were compacted into 71-mm (2.8-in.) diam. × 152-mm (6-in.) height. These soils are designated as subgrade soils, according to AASHTO TP46-94. The sample preparation procedure was similar to that developed by Baltzer and Irwin (1995). Details of the compaction study are provided in Appendix A.

The samples were compacted in five layers using a CS 1200 electrohydraulic kneading compactor manufactured by James Cox & Sons, Inc. (Fig. 3). This kneading compactor can be programmed for pressure–time curves, repetition of rates, ex-

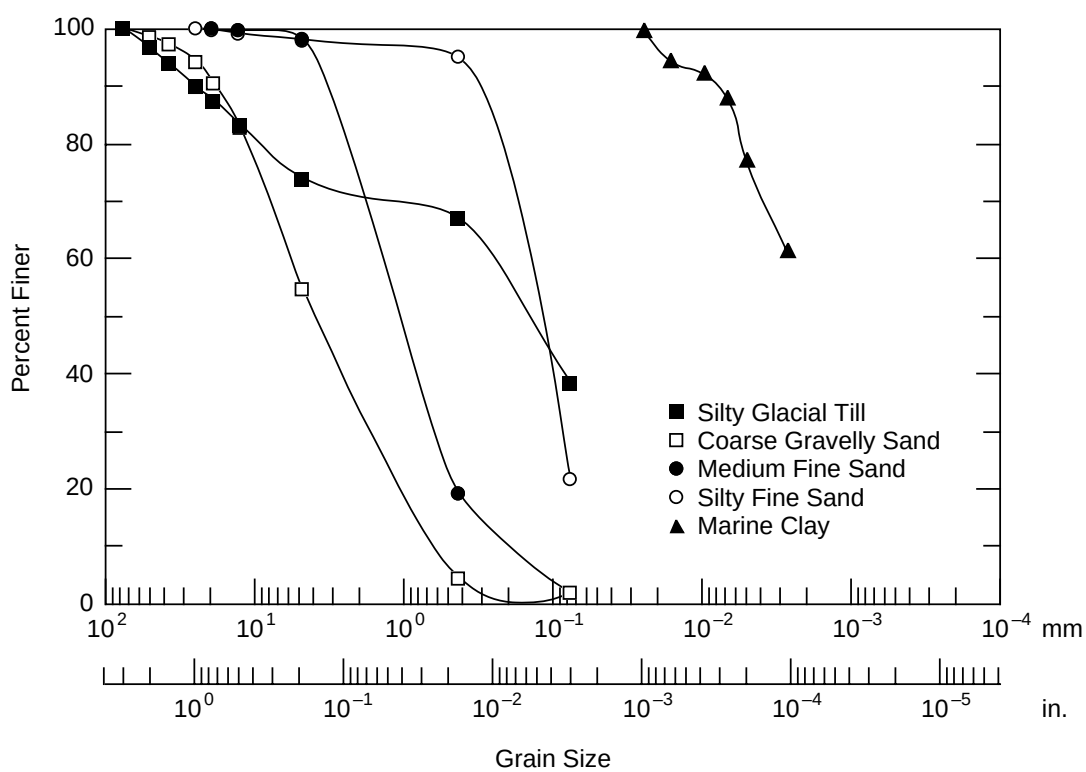

Figure 2. Grain size distribution for test soils.

Table 1. Classification properties of test soils.

CRREL designation	Classification: New Hampshire	Classification: AASHTO	Classification: USCS	Optimum moisture ω (%)	Density γ_d kg/m³ (pcf)
NH1	Silt, some fine sand. Some coarse to fine gravel, trace coarse to medium sand (glacial till).	A-4	SM	9.0	2050 (128)
NH2	Fine sand, some silt.	A-2-4	SM	14.5	1714 (107)
NH3	Coarse to fine gravelly, coarse to medium sand, trace fine sand.	A-1-a	SP	9.5	1730 (108)
NH4	Coarse to medium sand, little fine sand.	A-1-b	SP	13.6	1642 (102.5)
NH5	Clayey silt (marine deposit).	A-7-5	ML	23.5	1618 (101)

tended dwell times at peak pressure, and a variety of predetermined totals of compaction counts. It has been used at our laboratory for asphalt specimens, and was retrofitted to make the 2.8-in.-diam. and 6-in. soil samples. A procedure was developed (see App. A) to reproduce uniform density and moisture samples. The test specimens were fabricated at optimum moisture and density. This was accomplished by applying a known kneading pressure to the specimen through a tamping foot by means of a controlled dynamic force. As the kneading pressure was applied, the sample rotated on the compactor's rotating table. The rotation was electronically timed to the tamper foot.

A brief summary of the test method is presented here. Details on the sample preparation and testing method can be found in Appendix B. Vertical and radial deformations, confining pressure, deviator stresses and temperatures were measured during the test. Vertical deformations were measured using linear variable displacement transducers (LVDTs). Radial deformations were measured using non-contact variable inductance transducers (VITs). Three multi-VITs were used for the measurements. Temperature was measured using thermistors in dummy samples located in the environmental chamber. A typical setup is shown in Figure 4. For the resilient modulus tests, the temperatures used for testing ranged from room temperature +20°, +0.5°, –0.5°, –2°, –5°, and –10° C. The ±0.5 °C test temperatures were of particular interest for the thawing process. Several tests were conducted at –20°C, and we found that the resilient modulus was similar to that obtained at –10°C, except for the marine clay. Tests at –20°C were discontinued for all materials, with the exception of the marine clay. A minimum of two tests were conducted at each temperature.

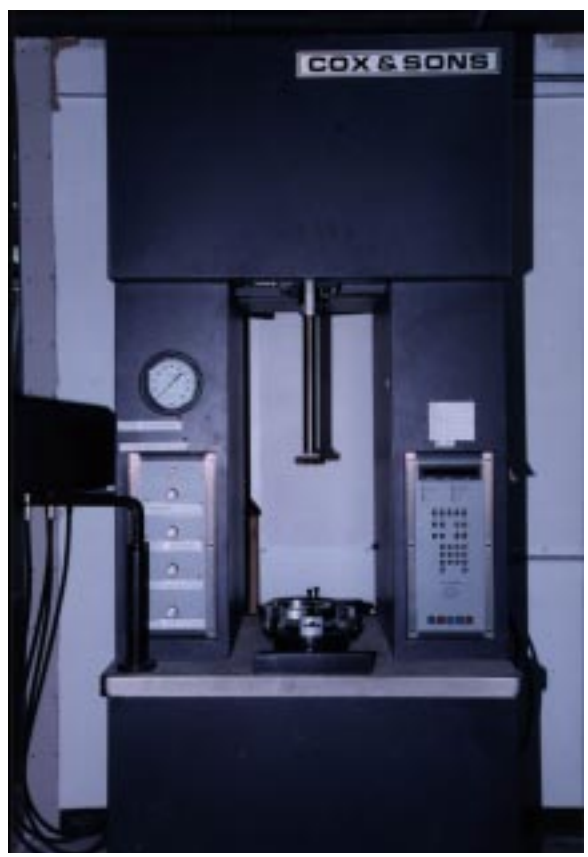

Figure 3. Kneading compactor used for fabricating test specimens.

Figure 4. Typical sample setup.

Table 2 shows the testing sequence used most of the time at the different temperatures. A description for the CRREL and AASHTO test methods are presented in Appendix B. The testing was done in a cycle. The samples were initially conditioned at room temperature and tested at room temperature. Then they were frozen and tested at the different frozen temperatures. The samples were thawed from –10°C to room temperature and tested at the intermediate temperatures.

Although most of the resilient modulus tests were conducted at optimum moisture content, a limited number were conducted at the saturated water content to determine the effect of moisture content. In addition, shear strength and hydrostatic tests were also conducted for some of the soils at the optimum water content. Table 3 shows the soil types, moisture content, density, and types of tests conducted. The test moisture and densities used were the optimum moistures and densities provided by NHDOT. The exception to the above is the coarse gravelly sand. For the coarse gravelly sand (NH3), we found that, when the specimens were compacted at the optimum moisture content (9.5%) provided by the NHDOT, the water drained rapidly and collected at the bottom of the specimen. For these samples, we continued making the specimens at 9.5% but allowed the water to drain before the beginning of the resilient modulus test. At the end of the test, the measured moisture content was approximately 3%.

RESULTS AND DISCUSSION

The discussion will focus on the results from the resilient modulus tests at optimum moisture content. There is insufficient information at this time to conclude on the effect of moisture content on the effective resilient modulus. As for the shear and hydrostatic tests (Tables 4 and 5), the results were planned to be used for predicting the amount of subgrade rutting during the spring thaw period. However, at this time additional testing is required.

Tables 6 to 10 present the resilient modulus results for the various soils as a function of temperature, confining pressure, and deviator stress. However, since the current AASHTO design uses a

Table 2. Testing sequence protocol used in the resilient modulus test.

Test temperature (°C)	*Subgrade material*	*Base/subbase material*
–10	CRREL	CRREL
–5	CRREL	CRREL
–2	CRREL / AASHTO (TP 46-94) – Table 1*	CRREL
–0.5	AASHTO (TP 46-94) – Table 1	AASHTO (TP 46-94) – Table 2
+0.5	AASHTO (TP 46-94) – Table 1	AASHTO (TP 46-94) – Table 2
+5	AASHTO (TP 46-94) – Table 1	AASHTO (TP 46-94) – Table 2
+20	AASHTO (TP 46-94) – Table 1	AASHTO (TP 46-94) – Table 2

*For the marine clay, AASHTO TP 46-94 Table 1 was used.

Table 3. Test conditions and types of tests.

CRREL designation	AASHTO	Test moisture/density		Resilient modulus		Shear	Hydrostatic compression
		ω (%)	γ_d kg/m³ (pcf)	Optimum	Saturated		
NH1	A-4	9	2050 (128)	√		√	√
NH2	A-2-4	14.5	1714 (107)	√			
NH3	A-1-a	9.5	1730 (108)	√		√	√
NH4	A-1-b	13.6	1642 (102.5)	√	√	√	√
NH5	A7-5	23.5	1618 (101)	√			

Table 4. Test temperatures for shear tests.

CRREL designation	Test temperature (°C)				
	20	0.5	–0.5	–2	20T
NH1	21, 34.5, 138* (3,5,20)			103, 138 (15,20)	
NH2					
NH3	138 (20)			138 (20)	138 (20)
NH4	69 (10)				

*Numbers in table are confining pressures in kPa (psi).

single value to represent the resilient modulus of the subgrade, the test values are averaged at each temperature and presented in Table 11 and graphically in Figures 5 to 9. Analysis of the effect of confining pressure, deviator stress, and temperature on the resilient modulus is presented by Simonsen et al. (in prep.). In all cases, as expected, the resilient modulus increases significantly when the temperature drops to below freezing. Observation of the results indicate that the rate of change is largest between 0° and –2°C for all soils during freezing and thawing. At temperatures below –2°C, the difference in the resilient modulus during freezing or thawing is minimal. However, close to 0°C, there are significant differences between the modulus obtained during the freezing and thawing process. There is a significant decrease (approximately 3.5 times less) in the resilient moduli of the clay and the fine sand after thaw and before freezing. It also appears never to regain strength. At positive temperatures, the resilient modulus remains constant.

It is well known that during the freezing and thawing process, the ground temperatures are higher or lower than the air temperatures. Using the mean air temperature to determine the monthly resilient modulus may produce significantly different moduli values. The FROST model (Guymon et al. 1993) was used to estimate the temperature at the top of the subgrade. The top of the subgrade was chosen since the current mechanistic model use the vertical strain at top of the subgrade as a failure criteria. Basically, the model is a one-dimensional vertical heat mass moisture

Table 5. Test temperatures for hydrostatic compression tests.

CRREL designation	Test temperature (°C)			
	20	0.5	–0.5	–2
NH1	√			√
NH2				
NH3				√
NH4	√			

Table 6. Resilient modulus test results for NH1.

			NH 1-5			*NH 1-4*		
Temp *°C*	σ_c *kPa (psi)*	*Max.* σ_1 *kPa (psi)*	ω *(%)*	γ_d *kg/m³ (pcf)*	M_r *MPa (psi)*	ω *(%)*	γ_d *kg/m³ (pcf)*	M_r *MPa (psi)*
20	41 (6)	14 (2)	8.9	2138 (133.5)	58 (8431)	8.9	2138 (133.5)	31 (4550)
20	41 (6)	28 (4)				8.9	2138 (133.5)	39 (5665)
20	28 (4)	14 (2)	8.9	2138 (133.5)	46 (6602)	8.9	2138 (133.5)	46 (6653)
5	41 (6)	14 (2)				8.9	2138 (133.5)	47 (6843)
5	41 (6)	28 (4)				8.9	2138 (133.5)	39 (5623)
5	28 (4)	14 (2)				8.9	2138 (133.5)	44 (6387)
0.5	41 (6)	14 (2)	8.9	2138 (133.5)	72 (10,470)	8.9	2138 (133.5)	52 (7519)
0.5	41 (6)	28 (4)	8.9	2138 (133.5)	66 (9532)	8.9	2138 (133.5)	49 (7147)
0.5	28 (4)	14 (2)	8.9	2138 (133.5)	50 (7196)	8.9	2138 (133.5)	35 (5056)
–0.5	138 (20)	117 (17)	8.9	2138 (133.5)	577 (83,723)			
–0.5	138 (20)	241 (35)	8.9	2138 (133.5)	493 (71,472)			
–0.5	103 (15)	117 (17)	8.9	2138 (133.5)	465 (67,410)			
–0.5	69 (10)	117 (17)	8.9	2138 (133.5)	464 (67,314)			
–0.5	34 (5)	117 (17)	8.9	2138 (133.5)	491 (71,220)			
–0.5	21 (3)	117 (17)	8.9	2138 (133.5)	493 (71,454)			
–2	138 (20)	117 (17)	8.9	2138 (133.5)	3727 (540,576)			
–2	138 (20)	241 (35)	8.9	2138 (133.5)	3477 (504,235)			
–2	138 (20)	476 (69)	8.9	2138 (133.5)	2836 (411,362)			
–2	138 (20)	717 (104)	8.9	2138 (133.5)	2379 (344,971)			
–2	103 (15)	241 (35)	8.9	2138 (133.5)	2469 (358,172)			
–2	103 (15)	476 (69)	8.9	2138 (133.5)	2911 (422,203)			
–2	103 (15)	717 (104)	8.9	2138 (133.5)	2502 (362,877)			
–2	69 (10)	241 (35)	8.9	2138 (133.5)	2411 (349,772)			
–2	69 (10)	476 (69)	8.9	2138 (133.5)	2656 (385,285)			
–2	69 (10)	717 (104)	8.9	2138 (133.5)	2388 (346,407)			
–2	34 (5)	241 (35)	8.9	2138 (133.5)	2414 (350,170)			
–2	34 (5)	476 (69)	8.9	2138 (133.5)	11,588 (1,680,664)			
–2	34 (5)	717 (104)	8.9	2138 (133.5)	9404 (1,363,997)			
–5	138 (20)	958 (139)	8.9	2138 (133.5)	8111 (1,176,455)			
–5	138 (20)	1434 (208)	8.9	2138 (133.5)	11,745 (1,703,464)			
–5	138 (20)	1917 (278)	8.9	2138 (133.5)	9145 (1,326,338)			
–5	103 (15)	958 (139)	8.9	2138 (133.5)	12,209 (1,770,660)			
–5	103 (15)	1434 (208)	8.9	2138 (133.5)	9198 (1,334,056)			
–5	69 (10)	958 (139)	8.9	2138 (133.5)	7765 (1,126,223)			
–5	69 (10)	1434 (208)	8.9	2138 (133.5)	11,267 (1,634,094)			
–5	69 (10)	1917 (278)	8.9	2138 (133.5)	8922 (1,294,109)			
–5	34 (5)	958 (139)	8.9	2138 (133.5)	7753 (1,124,494)			
–5	34 (5)	1434 (208)	8.9	2138 (133.5)	18,245 (2,646,071)			
–5	34 (5)	1917 (278)	8.9	2138 (133.5)	7753 (1,124,494)			
–10	138 (20)	958 (139)	8.9	2138 (133.5)	18,244 (2,646,071)			
–10	138 (20)	1434 (208)	8.9	2138 (133.5)	14,558 (2,111,326)			
–10	138 (20)	1917 (278)	8.9	2138 (133.5)	13,597 (1,972,043)			
–10	103 (15)	958 (139)	8.9	2138 (133.5)	19,731 (2,861,669)			
–10	103 (15)	1434 (208)	8.9	2138 (133.5)	15,365 (2,228,494)			
–10	103 (15)	1917 (278)	8.9	2138 (133.5)	12,958 (1,879,377)			
–10	69 (10)	958 (139)	8.9	2138 (133.5)	18,708 (2,713,277)			
–10	69 (10)	1434 (208)	8.9	2138 (133.5)	15,821 (2,294,596)			
–10	69 (10)	1917 (278)	8.9	2138 (133.5)	13,519 (1,960,694)			
20	41 (6)	14 (2)	8.9	2138 (133.5)	37 (5328)			
20	28 (4)	14 (2)	8.9	2138 (133.5)	38 (5574)			

Table 7. Resilient modulus test results for NH2.

			NH 2-3				*NH 2-4*			
Temp °C	σ_d *kPa (psi)*	*Max.* σ_1 *kPa (psi)*	ω *(%)*	γ_d *kg/m³ (pcf)*	μ	M_r *MPa (psi)*	ω *(%)*	γ_d *kg/m³ (pcf)*	μ	M_r *MPa (psi)*
20	41 (6)	14 (2)	10.3	1754 (110)	0.42	58 (8360)				
20	41 (6)	28 (4)	10.3	1754 (110)	0.64	68 (9836)				
20	41 (6)	41 (6)	10.3	1754 (110)	1.30	66 (9522)				
20	41 (6)	55 (8)	10.3	1754 (110)	1.40	63 (9101)				
20	28 (4)	14 (2)	10.3	1754 (110)	0.45	53 (7718)				
20	28 (4)	28 (4)	10.3	1754 (110)	0.79	57 (8238)				
20	14 (2)	14 (2)	10.3	1754 (110)	0.49	47 (6760)				
5.0	41 (6)	14 (2)	10.3	1754 (110)	0.40	57 (8237)	10.2	1759 (110)	0.49	59 (8629)
5.0	41 (6)	28 (4)	10.3	1754 (110)	0.52	64 (9289)	10.2	1759 (110)	0.56	71 (10,317)
5.0	28 (4)	14 (2)	10.3	1754 (110)	0.45	47 (6799)	10.2	1759 (110)	0.48	53 (7630)
5.0	28 (4)	28 (4)	10.3	1754 (110)	0.82	52 (7558)				
5.0	14 (2)	14 (2)					10.2	1759 (110)	0.47	48 (6900)
5.0	14 (2)	28 (4)	10.3	1754 (110)	0.46	42 (6126)				
0.5	41 (6)	14 (2)	10.3	1754 (110)	0.42	53 (7664)	10.2	1759 (110)	0.46	52 (7576)
0.5	41 (6)	28 (4)	10.3	1754 (110)		60 (8760)	10.2	1759 (110)		68 (9923)
0.5	28 (4)	14 (2)	10.3	1754 (110)	0.49	46 (6744)	10.2	1759 (110)	0.46	48 (6928)
0.5	28 (4)	28 (4)	10.3	1754 (110)		52 (7500)				
0.5	14 (2)	14 (2)					10.2	1759 (110)	0.50	45 (6577)
0.5	14 (2)	28 (4)	10.3	1754 (110)	0.45	41 (5922)				
–0.5	41 (6)	14 (2)					10.2	1759 (110)	0.26	205 (29,777)
–0.5	41 (6)	28 (4)	10.3	1754 (110)		507 (73,462)	10.2	1759 (110)	0.33	210 (30,499)
–0.5	41 (6)	41 (6)	10.3	1754 (110)	0.49	465 (67,383)	10.2	1759 (110)	0.31	196 (28,459)
–0.5	41 (6)	55 (8)	10.3	1754 (110)	0.43	391 (56,760)	10.2	1759 (110)	0.30	198 (28,683)
–0.5	41 (6)	69 (10)	10.3	1754 (110)	0.39	382 (55,364)				
–0.5	28 (4)	14 (2)					10.2	1759 (110)	0.31	196 (28,491)
–0.5	28 (4)	28 (4)	10.3		0.50	439 (63,655)	10.2	1759 (110)	0.33	183 (26,595)
–0.5	28 (4)	41 (6)	10.3	1754 (110)	0.35	402 (58,329)	10.2	1759 (110)	0.32	185 (26,806)
–0.5	28 (4)	55 (8)	10.3		0.31	366 (53,075)	10.2	1759 (110)	0.31	190 (27,570)
–0.5	28 (4)	69 (10)	10.3	1754 (110)	0.34	374 (54,264)				
–0.5	14 (2)	14 (2)					10.2	1759 (110)		205 (29,772)
–0.5	14 (2)	28 (4)	10.3	1754 (110)	0.42	389 (56,356)	10.2	1759 (110)	0.27	175 (25,437)
–0.5	14 (2)	41 (6)	10.3		0.42	396 (57,482)	10.2	1759 (110)	0.23	183 (26,482)
–0.5	14 (2)	55 (8)	10.3	1754 (110)	0.27	369 (53,485)	10.2	1759 (110)	0.40	192 (27,813)
–0.5	14 (2)	69 (10)	10.3		0.41	369 (53,447)				
–2.0	69 (10)	448 (65)	10.3	1754 (110)	0.14	3364 (487,847)	10.2	1759 (110)	0.37	3621 (525,135)
–2.0	55 (8)	448 (65)	10.3	1754 (110)	0.13	3301 (478,741)	10.2	1759 (110)		4021 (583,256)
–2.0	41 (6)	448 (65)	10.3	1754 (110)	0.18	3225 (467,808)	10.2	1759 (110)	0.27	3978 (576,974)
–5.0	69 (10)	896 (130)	10.3	1754 (110)	0.34	6192 (898,045)	10.2	1759 (110)		5223 (757,512)
–5.0	55 (8)	896 (130)	10.3	1754 (110)	0.35	6447 (935,070)	10.2	1759 (110)		7319 (1,061,522)
–5.0	41 (6)	896 (130)	10.3	1754 (110)	0.28	6280 (910,797)	10.2	1759 (110)		5581 (809,480)
–10.0	69 (10)	896 (130)					10.2	1759 (110)		10,309 (1,495,137)
–10.0	55 (8)	896 (130)					10.2	1759 (110)		10,800 (1,566,390)
–10.0	41 (6)	896 (130)	10.3	1754 (110)	0.27	10,241 (1,485,291)	10.2	1759 (110)		11,542 (1,674,089)
–5.0	69 (10)	896 (130)	10.3	1754 (110)	0.43	6489 (941,187)	10.2	1759 (110)		7375 (1,069,708)
–5.0	55 (8)	896 (130)	10.3	1754 (110)	0.39	6190 (897,775)	10.2	1759 (110)	0.40	7649 (1,109,461)
–5.0	41 (6)	896 (130)	10.3	1754 (110)	0.40	6451 (935,683)	10.2	1759 (110)	0.38	7432 (1,077,928)
–2.0	69 (10)	448 (65)	10.3	1754 (110)	0.40	3360 (487,271)	10.2	1759 (110)	0.36	4518 (655,283)
–2.0	41 (6)	448 (65)	10.3	1754 (110)	0.47	3376 (489,609)	10.2	1759 (110)	0.41	4407 (639,228)
–0.5	41 (6)	28 (4)	10.3	1754 (110)	0.39	699 (101,448)	10.2	1759 (110)	0.33	696 (100,912)
–0.5	41 (6)	41 (6)	10.3	1754 (110)		619 (89,748)	10.2	1759 (110)	0.43	613 (88,979)
–0.5	41 (6)	55 (8)	10.3	1754 (110)	0.38	529 (76,733)	10.2	1759 (110)	0.50	596 (86,421)
–0.5	41 (6)	69 (10)	10.3	1754 (110)	0.43	506 (73,427)	10.2	1759 (110)	0.47	583 (84,560)
–0.5	28 (4)	14 (2)					10.2	1759 (110)		750 (108,845)
–0.5	28 (4)	28 (4)	10.3	1754 (110)		622 (90,220)	10.2	1759 (110)	0.50	625 (90,638)
–0.5	28 (4)	41 (6)	10.3	1754 (110)	0.42	547 (79,265)	10.2	1759 (110)		578 (83,761)
–0.5	28 (4)	55 (8)	10.3	1754 (110)	0.50	513 (74,467)	10.2	1759 (110)	0.43	535 (77,590)

Table 7 (cont'd). Resilient modulus test results for NH2.

			NH 2-3				NH 2-4			
Temp °C	σ_c *kPa (psi)*	*Max.* σ_1 *kPa (psi)*	ω *(%)*	γ_d *kg/m³ (pcf)*	μ	M_r *MPa (psi)*	ω *(%)*	γ_d *kg/m³ (pcf)*	μ	M_r *MPa (psi)*
–0.5	28 (4)	69 (10)	10.3	1754 (110)	0.34	511 (74,098)	10.2	1759 (110)		558 (80,958)
–0.5	14 (2)	14 (2)					10.2	1759 (110)		705 (102,206)
–0.5	14 (2)	28 (4)	10.3	1754 (110)	0.36	375 (54,382)	10.2	1759 (110)	0.26	617 (89,470)
–0.5	14 (2)	41 (6)	10.3	1754 (110)		646 (93,687)	10.2	1759 (110)		609 (88,298)
–0.5	14 (2)	55 (8)	10.3	1754 (110)		569 (82,532)	10.2	1759 (110)		555 (80,501)
–0.5	14 (2)	69 (10)	10.3	1754 (110)	0.41	368 (53,420)	10.2	1759 (110)	0.38	534 (77,463)
0.5	41 (6)	14 (2)					10.2	1759 (110)	0.50	54 (7805)
0.5	41 (6)	28 (4)	10.3	1754 (110)		50 (7282)	10.2	1759 (110)		61 (8850)
0.5	41 (6)	41 (6)	10.3	1754 (110)		55 (7958)				
0.5	41 (6)	14 (2)					10.2	1759 (110)	0.50	54 (7805)
0.5	41 (6)	28 (4)	10.3	1754 (110)		50 (7282)	10.2	1759 (110)		61 (8850)
0.5	41 (6)	41 (6)	10.3	1754 (110)		55 (7958)				
0.5	28 (4)	14 (2)	10.3	1754 (110)		43 (6307)	10.2	1759 (110)	0.50	47 (6745)
0.5	14 (2)	14 (2)	10.3	1754 (110)		41 (5956)	10.2	1759 (110)		44 (6422)
20	41 (6)	14 (2)	10.3	1754 (110)		48 (7018)				
20	41 (6)	28 (4)	10.3	1754 (110)		59 (8570)				
20	28 (4)	14 (2)	10.3	1754 (110)		44 (6324)				
20	14 (2)	14 (2)	10.3	1754 (110)		41 (6013)				

flow model that is primarily used for calculating frost heave. As part of the frost heave calculations, the model calculates the temperature, moisture content, etc., in the base and subgrade as a function of time.

The following typical pavement structures were used in the analysis. For interstate and primary pavement structures, there was 152 mm (6 in.) asphalt concrete, over 610 mm (24 in.) of base, over 305 mm (12 in.) of subbase, over the various subgrades. For secondary roads, there was 76 mm (3 in.) of asphalt concrete, over 406 mm (16 in.) of base, over 203 mm (8 in.) of subbase, over the subgrades (Fig. 10). The base layer in this analysis is the combination of the crushed gravel and gravel layers. The CRREL soil database was used to estimate the thermal and hydraulic properties of the various pavement layers. For the base, subbase, and subgrade, selection was based on the gradation of the material. The minimum and maximum air temperatures, based on 30 years of record were used to calculate the annual air freezing index (AFI). The design freezing index (DFI) is the average of the three coldest years. The air temperatures at Concord and Lebanon were used for the analysis (Fig. 11). Once, the DFI is calculated for both locations, the closest air freezing index was chosen as the design air temperature for each site respectively. It was found that the difference between the calculated subgrade temperatures at Concord and Lebanon were similar. The air and top of the subgrade temperatures for Concord are shown in Figures 12 and 13. As seen in Figures 11 and 12, even though the mean air temperature during the winter was around –10°C, the minimum subgrade temperature was around 0° and –3°C. These results are probably applicable to all parts of the state, except at locations in the higher elevations. The mean air and top of subgrade temperatures under interstate and secondary highway pavements are presented in Table 12.

The mean temperatures in Table 12 were used in most cases for determining the resilient modulus. However, during the late winter early spring periods, there is a rapid change of temperature, Fig. 14a and b. For example, for the first half of March, the subgrade temperature is on an average around –3°C. The temperature for the remaining part of the month hovers around 0°C. In these instances, two temperatures are used to estimate the resilient moduli for the month of March (Table 13).

The calculations for the effective resilient modulus for the various subgrade soils are presented in Table 14 and are summarized in Table 15. The resilient modulus values in Table 14 were obtained by straight line interpolation between the temperatures in Figures 5 to 9. The relative damage (u_f) in

Table 8a. Resilient modulus test results for NH3.

			NH 3-1				*NH 3-3*			
Temp °C	σ_c *kPa (psi)*	*Max.* σ_1 *kPa (psi)*	ω *(%)*	γ_d *kg/m³ (pcf)*	μ	M_r *MPa (psi)*	ω *(%)*	γ_d *kg/m³ (pcf)*	μ	M_r *MPa (psi)*
20	138 (20)	14 (2)	drained	1930 (121)		395 (57,257)				
20	138 (20)	28 (4)	drained	1930 (121)		389 (56,363)	1.6	1930 (121)	0.45	284 (41,152)
20	138 (20)	41 (6)	drained	1930 (121)		353 (51,249)				
20	138 (20)	55 (8)	drained	1930 (121)		347 (50,278)	1.6	1930 (121)	0.42	278 (40,263)
20	138 (20)	69 (10)	drained	1930 (121)		338 (49,083)	1.6	1930 (121)	0.35	286 (41,527)
20	138 (20)	83 (12)	drained	1930 (121)		329 (47,711)				
20	138 (20)	103 (15)	drained	1930 (121)		326 (47,259)	1.6	1930 (121)	0.27	285 (41,342)
20	138 (20)	138 (20)	drained	1930 (121)		322 (46,759)	1.6	1930 (121)	0.30	286 (41,527)
0.5	138 (20)	28 (4)					1.6	1930 (121)	0.34	321 (46,625)
0.5	138 (20)	55 (8)					1.6	1930 (121)	0.31	307 (44,522)
0.5	138 (20)	69 (10)					1.6	1930 (121)	0.18	310 (45,028)
0.5	138 (20)	103 (15)					1.6	1930 (121)	0.26	315 (45,647)
0.5	138 (20)	138 (20)					1.6	1930 (121)	0.29	317 (45,980)
0.5	138 (20)	207 (30)					1.6	1930 (121)	0.40	322 (46,734)
–0.5	138 (20)	28 (4)	drained	1930 (121)	0.30	329 (47,747)	1.6	1930 (121)		414 (59,992)
–0.5	138 (20)	55 (8)	drained	1930 (121)	0.36	325 (47,120)	1.6	1930 (121)	0.26	346 (50,238)
–0.5	138 (20)	69 (10)	drained	1930 (121)	0.39	328 (47,632)	1.6	1930 (121)	0.32	335 (48,574)
–0.5	138 (20)	103 (15)	drained	1930 (121)	0.39	322 (46,737)	1.6	1930 (121)	0.29	335 (48,625)
–0.5	138 (20)	138 (20)	drained	1930 (121)	0.41	327 (47,415)	1.6	1930 (121)	0.29	344 (49,881)
–0.5	138 (20)	207 (30)					1.6	1930 (121)	0.35	362 (52,466)
–0.5	138 (20)	276 (40)					1.6	1930 (121)	0.41	382 (55,372)
–2	138 (20)	28 (4)	drained	1930 (121)		3567 (517,359)				
–2	138 (20)	55 (8)	drained	1930 (121)		4921 (713,721)				
–2	138 (20)	69 (10)	drained	1930 (121)		5406 (784,009)	1.6	1930 (121)		2500 (362,641)
–2	138 (20)	103 (15)	drained	1930 (121)		5681 (823,997)				
–2	138 (20)	138 (20)	drained	1930 (121)		5042 (731,247)	1.6	1930 (121)		2331 (338,055)
–2	138 (20)	207 (30)	drained	1930 (121)		4445 (644,661)	1.6	1930 (121)		2179 (316,016)
–2	138 (20)	276 (40)	drained	1930 (121)		4197 (608,749)	1.6	1930 (121)		2104 (305,181)
–2	138 (20)	345 (50)	drained	1930 (121)		3922 (568,789)	1.6	1930 (121)	0.46	2074 (300,875)
–5	138 (20)	55 (8)	drained	1930 (121)		3688 (534,873)	1.6	1930 (121)		2453 (355,789)
–5	138 (20)	69 (10)	drained	1930 (121)		5146 (746,306)	1.6	1930 (121)		2263 (328,235)
–5	138 (20)	103 (15)	drained	1930 (121)		4820 (699,045)	1.6	1930 (121)		2312 (335,399)
–5	138 (20)	138 (20)	drained	1930 (121)		5236 (759,427)	1.6	1930 (121)		2293 (332,515)
–5	138 (20)	207 (30)	drained	1930 (121)		4300 (623,661)	1.6	1930 (121)	0.39	2458 (356,513)
–5	138 (20)	276 (40)	drained	1930 (121)		3998 (579,812)				
–5	138 (20)	345 (50)	drained	1930 (121)		3708 (537,778)				
–10	138 (20)	69 (10)	drained	1930 (121)		3807 (552,102)	1.6	1930 (121)		2691 (390,224)
–10	138 (20)	103 (15)	drained	1930 (121)		3828 (555,233)				
–10	138 (20)	138 (20)	drained	1930 (121)		3668 (532,024)	1.6	1930 (121)		2942 (426,705)
–10	138 (20)	207 (30)	drained	1930 (121)		3607 (523,082)	1.6	1930 (121)		2622 (380,225)
–10	138 (20)	276 (40)	drained	1930 (121)		3439 (498,845)	1.6	1930 (121)		2577 (373,824)
–10	138 (20)	345 (50)	drained	1930 (121)	0.42	3331 (483,141)	1.6	1930 (121)		2591 (375,765)
–10	138 (20)	55 (8)	drained	1930 (121)		4603 (667,547)				
–10	138 (20)	69 (10)	drained	1930 (121)		3190 (462,655)				
–10	138 (20)	103 (15)	drained	1930 (121)		3372 (489,088)				
–10	138 (20)	138 (20)	drained	1930 (121)		3334 (483,524)				
–10	138 (20)	207 (30)	drained	1930 (121)		3238 (469,641)				
–10	138 (20)	276 (40)	drained	1930 (121)		3156 (457,776)				
–10	138 (20)	345 (50)	drained	1930 (121)		3185 (461,948)				
–5	138 (20)	55 (8)	drained	1930 (121)		4352 (631,270)				
–5	138 (20)	69 (10)	drained	1930 (121)		3577 (518,823)	1.6	1930 (121)		3223 (467,468)
–5	138 (20)	138 (20)	drained	1930 (121)		2788 (404,414)	1.6	1930 (121)		2808 (407,316)
–5	138 (20)	207 (30)	drained	1930 (121)		2896 (420,018)	1.6	1930 (121)		2606 (378,000)
–5	138 (20)	276 (40)	drained	1930 (121)		2764 (400,939)	1.6	1930 (121)		2475 (359,000)

Table 8a (cont'd). Resilient modulus test results for NH3.

			NH 3-1				NH 3-3			
Temp *°C*	σ_c *kPa (psi)*	*Max.* σ_1 *kPa (psi)*	ω *(%)*	γ_d *kg/m³ (pcf)*	μ	M_r *MPa (psi)*	ω *(%)*	γ_d *kg/m³ (pcf)*	μ	M_r *MPa (psi)*
–5	138 (20)	345 (50)	drained	1930 (121)		2742 (397,698)	1.6	1930 (121)		2472 (358,596)
–2	138 (20)	55 (8)	drained	1930 (121)		2630 (381,458)				
–2	138 (20)	69 (10)	drained	1930 (121)		2782 (403,439)	1.6	1930 (121)		2883 (418,084)
–2	138 (20)	138 (20)	drained	1930 (121)	0.43	2113 (306,415)	1.6	1930 (121)		2130 (308,945)
–2	138 (20)	207 (30)	drained	1930 (121)	0.43	1866 (270,604)	1.6	1930 (121)		2027 (294,009)
–2	138 (20)	276 (40)	drained	1930 (121)	0.35	1825 (264,631)	1.6	1930 (121)		1998 (289,741)
–2	138 (20)	345 (50)	drained	1930 (121)	0.36	1840 (266,804)	1.6	1930 (121)		1931 (280,137)
–0.5	138 (20)	28 (4)	drained	1930 (121)		1443 (209,284)				
–0.5	138 (20)	55 (8)	drained	1930 (121)		1329 (192,732)	1.6	1930 (121)		1258 (182,472)
–0.5	138 (20)	69 (10)	drained	1930 (121)		1318 (191,133)	1.6	1930 (121)		1341 (194,520)
–0.5	138 (20)	103 (15)	drained	1930 (121)		1270 (184,170)				
–0.5	138 (20)	138 (20)	drained	1930 (121)		1199 (173,895)	1.6	1930 (121)	0.4	1205 (174,771)
–0.5	138 (20)	207 (30)					1.6	1930 (121)	0.3	1222 (177,231)
–0.5	138 (20)	276 (40)					1.6	1930 (121)	0.3	1128 (163,583)
–0.5	138 (20)	345 (50)					1.6	1930 (121)	0.3	1084 (157,284)
0.5	138 (20)	28 (4)					1.6	1930 (121)		423 (61,360)
0.5	138 (20)	55 (8)					1.6	1930 (121)	0.3	265 (38,475)
0.5	138 (20)	69 (10)					1.6	1930 (121)	0.3	275 (39,845)
0.5	138 (20)	103 (15)					1.6	1930 (121)	0.4	279 (40,454)
0.5	138 (20)	138 (20)					1.6	1930 (121)	0.4	290 (42,007)
0.5	138 (20)	207 (30)					1.6	1930 (121)	0.4	319 (46,233)
20	138 (20)	14 (2)	drained	1930 (121)		244 (35,319)	-			
20	138 (20)	28 (4)	drained	1930 (121)		200 (29,020)	1.6	1930 (121)		203 (29,471)
20	138 (20)	55 (8)	drained	1930 (121)		201 (29,201)	1.6	1930 (121)	0.3	207 (30,018)
20	138 (20)	69 (10)	drained	1930 (121)		207 (29,965)	1.6	1930 (121)	0.3	220 (31,849)
20	138 (20)	83 (12)	drained	1930 (121)		214 (31,081)				
20	138 (20)	103 (15)	drained	1930 (121)		215 (31,140)	1.6	1930 (121)	0.3	225 (32,699)
20	138 (20)	138 (20)	drained	1930 (121)		230 (33,361)	1.6	1930 (121)	0.3	243 (35,278)

Table 8b. Resilient modulus for NH3 at room temperature.

			NH 3-4				NH 3-5			
Temp *°C*	σ_c *kPa (psi)*	*Max.* σ_1 *kPa (psi)*	ω *(%)*	γ_d *kg/m³ (pcf)*	μ	M_r *MPa (psi)*	ω *(%)*	γ_d *kg/m³ (pcf)*	μ	M_r *MPa (psi)*
20	28 (4)	138 (20)	2.1	1930 (121)		305 (44,218)	1.5		0.5	309 (44,817)
20	55 (8)	138 (20)	2.1	1930 (121)	0.28	322 (46,772)	1.5		0.3	316 (45,807)
20	69 (10)	138 (20)	2.1	1930 (121)	0.39	320 (46,344)	1.5		0.3	322 (46,654)
20	103 (15)	138 (20)	2.1	1930 (121)	0.36	315 (45,713)	1.5		0.2	319 (46,258)
20	138 (20)	138 (20)	2.1	1930 (121)	0.23	315 (45,618)	1.5		0.2	317 (45,980)
15	34 (5)	138 (20)	2.1	1930 (121)		268 (38,827)	1.5		0.4	241 (34,971)
15	69 (10)	138 (20)	2.1	1930 (121)	0.39	264 (38,241)	1.5		0.3	258 (37,366)
15	103 (15)	138 (20)	2.1	1930 (121)	0.26	264 (38,293)	1.5		0.3	256 (37,186)
15	138 (20)	138 (20)	2.1	1930 (121)	0.32	271 (39,249)	1.5		0.3	270 (39,089)
10	34 (5)	138 (20)	2.1	1930 (121)	0.50	198 (28,681)	1.5		0.3	192 (27,913)
10	103 (15)	138 (20)	2.1	1930 (121)	0.34	216 (31,294)	1.5		0.3	197 (28,555)
10	138 (20)	138 (20)	2.1	1930 (121)	0.41	226 (32,751)	1.5		0.3	206 (29,923)
5	34 (5)	138 (20)	2.1	1930 (121)	0.37	106 (15,386)	1.5		0.4	128 (18,555)
5	69 (10)	138 (20)	2.1	1930 (121)	0.46	129 (18,769)	1.5		0.4	147 (21,280)
5	103 (15)	138 (20)					1.5			158 (22,890)

Table 9. Resilient modulus test results for NH4.

			NH 4-1				*NH 4-2*			
Temp °C	σ_c *kPa (psi)*	*Max.* σ_1 *kPa (psi)*	ω *(%)*	γ_d *kg/m³ (pcf)*	μ	M_r *MPa (psi)*	ω *(%)*	γ_d *kg/m³ (pcf)*	μ	M_r *MPa (psi)*
5.0	41 (6)	14 (2)	14	1664 (104)		43 (6217)				
5.0	28 (4)	28 (4)	14	1664 (104)		27 (3942)				
0.5	41 (6)	14 (2)	14	1664 (104)		39 (5645)	13.8			52 (7555)
0.5	28 (4)	14 (2)	14	1664 (104)		28 (3990)	13.8			32 (4642)
–0.5	41 (6)	14 (2)	14	1664 (104)		106 (15,358)				
–0.5	41 (6)	28 (4)	14	1664 (104)		120 (17,465)				
–0.5	41 (6)	41 (6)	14	1664 (104)		133 (19,307)				
–2.0	69 (10)	138 (20)					13.8			8391 (1,216,990)
–2.0	69 (10)	207 (30)					13.8			6471 (938,503)
–2.0	69 (10)	338 (49)					13.8		0.4	6190 (897,832)
–2.0	69 (10)	448 (65)	14	1664 (104)		12,267 (1,779,241)				
–2.0	55 (8)	338 (49)					13.8		0.4	13,668 (1,982,442)
–2.0	55 (8)	448 (65)	14	1664 (104)		15,260 (2,213,203)				
–2.0	41 (6)	338 (49)					13.8			13,440 (1,949,267)
–2.0	41 (6)	448 (65)	14	1664 (104)	0.27	14,698 (2,131,765)				
–5.0	69 (10)	207 (30)								
–5.0	69 (10)	338 (49)					13.8		0.3	10,323 (1,497,186)
–5.0		448 (65)	14	1664 (104)		22,616 (3,280,167)				
–5.0		669 (97)	14	1664 (104)	1.47	18,018 (2,613,270)				
–5.0		896 (130)	14	1664 (104)	1.13	17,892 (2,595,071)				
–10.0	69 (10)	338 (49)								15,791 (2,290,248)
–10.0	69 (10)	448 (65)	14	1664 (104)		24,437 (3,544,313)				
–10.0	69 (10)	558 (81)						1690 (106)	0.7	15,286 (2,217,024)
–10.0	69 (10)	669 (97)	14	1664 (104)		23,305 (3,380,076)		1690 (106)	0.4	15,733 (2,281,814)
–10.0	69 (10)	896 (130)	14	1664 (104)		20,647 (2,994,602)				
–10.0	69 (10)	338 (49)						1690 (106)	1.8	24,900 (3,611,412)
–20.0	69 (10)	558 (81)						1690 (106)	0.8	16,673 (2,418,245)
–20.0	69 (10)	669 (97)						1690 (106)	0.6	17,227 (2,498,625)
–5.0	69 (10)	448 (65)	14	1664 (104)		25,557 (3,706,795)				
–5.0	69 (10)	669 (97)	14	1664 (104)		18,018 (2,613,270)				
–5.0	69 (10)	896 (130)	14	1664 (104)		16,107 (2,336,115)				
–2.0	69 (10)	338 (49)						1690 (106)		16,132 (2,339,703)
–2.0	69 (10)	448 (65)	14	1664 (104)		15,357 (2,227,413)				
–2.0	69 (10)	558 (81)						1690 (106)		16,735 (2,427,200)
–2.0	69 (10)	669 (97)						1690 (106)	0.4	15,838 (2,297,082)
–2.0	55 (8)	338 (49)						1690 (106)	0.1	12,984 (1,883,219)
–2.0	55 (8)	448 (65)	14	1664 (104)		15,260 (2,213,203)
–2.0	41 (6)	338 (49)						1690 (106)		8857 (1,284,538)
–2.0	41 (6)	448 (65)	14	1664 (104)		13,252 (1,922,041)				
–0.5	69 (10)	338 (49)						1690 (106)		8894 (1,289,898)
–0.5	41 (6)	221 (32)	14	1664 (104)		5341 (774,577)				
–0.5	41 (6)	338 (49)	14	1664 (104)		4871 (706,424)				
–0.5	41 (6)	448 (65)	14	1664 (104)	0.49	4815 (698,387)				
0.5	41 (6)	14 (2)	14	1664 (104)		14 (2018)	13.8	1690 (106)		10,592 (1,536,238)
0.5	41 (6)	28 (4)	14	1664 (104)		15 (2197)	13.8	1690 (106)		6307 (914,822)
0.5	41 (6)	41 (6)					13.8	1690 (106)	0.4	6390 (926,822)
0.5	28 (4)	28 (4)					13.8	1690 (106)	0.4	60 (8769)
0.5	14 (2)	28 (4)					13.8	1690 (106)	0.4	65 (9405)
5.0	28 (4)	14 (2)	14	1664 (104)		10 (1487)				
5.0	14 (2)	14 (2)	14	1664 (104)		10 (1476)				

Table 10. Resilient modulus test results for NH5.

			NH 5-1				*NH 5-2*			
Temp *°C*	σ_c *kPa (psi)*	*Max.* σ_1 *kPa (psi)*	ω *(%)*	γ_d *kg/m³ (pcf)*	μ	M_r *MPa (psi)*	ω *(%)*	γ_d *kg/m³ (pcf)*	μ	M_r *MPa (psi)*
5.0	41 (6)	14 (2)	23	1669 (104)	0.39	59 (8518)	23.8	1664 (104)	0.4	60 (8699)
5.0	41 (6)	28 (4)	23	1669 (104)	0.40	34 (4905)	23.8	1664 (104)	0.4	36 (5257)
5.0	28 (4)	14 (2)	23	1669 (104)	0.41	45 (6473)	23.8	1664 (104)	0.4	48 (6917)
0.5	41 (6)	14 (2)	23	1669 (104)	0.42	57 (8327)	23.8	1664 (104)	0.4	73 (10,547)
0.5	41 (6)	28 (4)	23	1669 (104)	0.39	39 (5725)	23.8	1664 (104)	0.4	40 (5759)
0.5	28 (4)	14 (2)	23	1669 (104)	0.39	51 (7356)	23.8	1664 (104)	0.4	51 (7380)
–0.5	41 (6)	14 (2)	23	1669 (104)	0.45	35 (5010)	23.8	1664 (104)	0.4	55 (8016)
–0.5	41 (6)	28 (4)					23.8	1664 (104)	0.4	39 (5584)
–0.5	28 (4)	14 (2)	23	1669 (104)	0.48	31 (4493)	23.8	1664 (104)	0.5	50 (7222)
–2.0	41 (6)	14 (2)	23	1669 (104)		296 (42,874)				
–2.0	41 (6)	28 (4)	23	1669 (104)		185 (26,796)				
–2.0	41 (6)	41 (6)	23	1669 (104)		141 (20,463)	23.8	1664 (104)		231 (33,529)
–2.0	28 (4)	14 (2)	23	1669 (104)		332 (48,172)				
–2.0	28 (4)	28 (4)	23	1669 (104)		179 (25,942)	23.8	1664 (104)		256 (37,197)
–2.0	28 (4)	41 (6)	23	1669 (104)		140 (20,248)	23.8	1664 (104)		233 (33,752)
–2.0	14 (2)	14 (2)	23	1669 (104)		273 (39,539)				
–2.0	14 (2)	28 (4)	23	1669 (104)		172 (24,924)	23.8	1664 (104)		253 (36,659)
–2.0	14 (2)	41 (6)	23	1669 (104)		139 (20,193)	23.8	1664 (104)		247 (35,866)
–5.0	69 (10)	138 (20)	23	1669 (104)	0.19	894 (129,651)	23.8	1664 (104)		1422 (206,262)
–5.0	69 (10)	207 (30)	23	1669 (104)	0.13	927 (134,424)	23.8	1664 (104)		1329 (192,737)
–10.0	69 (10)	103 (15)	23	1669 (104)		2200 (319,030)	-			
–10.0	69 (10)	221 (32)	23	1669 (104)		2548 (369,528)	23.8	1664 (104)		3641 (528,014)
–10.0	69 (10)	338 (49)	23	1669 (104)	0.40	2770 (401,691)	23.8	1664 (104)	0.3	3378 (489,988)
–10.0	69 (10)	448 (65)	23	1669 (104)	0.35	2800 (406,153)	23.8	1664 (104)	0.4	3135 (454,730)
–10.0	69 (10)	558 (81)	23	1669 (104)	0.38	2980 (432,189)	23.8	1664 (104)	0.4	3054 (442,943)
–10.0	69 (10)	669 (97)	23	1669 (104)	0.38	2755 (399,612)	23.8	1664 (104)	0.4	2797 (405,703)
–10.0	69 (10)	896 (130)	23	1669 (104)	0.32	2516 (364,940)	23.8	1664 (104)	0.4	2411 (349,725)
–20.0	69 (10)	448 (65)	23	1669 (104)	0.33	4913 (712,606)	23.8	1664 (104)	0.3	5812 (842,888)
–20.0	69 (10)	669 (97)	23	1669 (104)		5261 (762,979)	23.8	1664 (104)	0.3	5506 (798,524)
–20.0	69 (10)	896 (130)	23	1669 (104)	0.33	5358 (777,124)	23.8	1664 (104)	0.3	5161 (748,487)
–10.0	69 (10)	221 (32)	23	1669 (104)	0.47	2851 (413,469)	23.8	1664 (104)		3663 (531,204)
–10.0	69 (10)	338 (49)	23	1669 (104)	0.32	2940 (426,446)	23.8	1664 (104)		3520 (510,603)
–10.0	69 (10)	448 (65)	23	1669 (104)	0.21	2934 (425,536)	23.8	1664 (104)	0.4	3391 (491,766)
–10.0	69 (10)	558 (81)					23.8	1664 (104)	0.4	3248 (471,122)
–10.0	69 (10)	669 (97)	23	1669 (104)	0.50	3174 (460,381)	23.8	1664 (104)	0.4	2976 (431,673)
–10.0	69 (10)	896 (130)	23	1669 (104)		2925 (424,189)	23.8	1664 (104)	0.4	2690 (390,156)
–5.0	69 (10)	138 (20)	23	1669 (104)	0.18	1288 (186,785)	23.8	1664 (104)		1937 (280,989)
–5.0	69 (10)	207 (30)	23	1669 (104)	0.21	1302 (188,904)	23.8	1664 (104)		1816 (263,328)
–2.0	41 (6)	14 (2)	23	1669 (104)		198 (28,725)	23.8	1664 (104)		104 (15,132)
–2.0	41 (6)	28 (4)	23	1669 (104)	0.31	136 (19,765)	23.8	1664 (104)		72 (10,445)
–2.0	41 (6)	41 (6)	23	1669 (104)		102 (14,722)	23.8	1664 (104)		55 (7970)
–2.0	28 (4)	14 (2)	23	1669 (104)	0.18	139 (20,182)	23.8	1664 (104)		115 (16,610)
–2.0	28 (4)	28 (4)	23	1669 (104)		99 (14,353)	23.8	1664 (104)		66 (9613)
–2.0	28 (4)	41 (6)					23.8	1664 (104)		56 (8083)
–2.0	14 (2)	14 (2)	23	1669 (104)	0.10	132 (19,165)	23.8	1664 (104)		117 (17,008)
–2.0	14 (2)	28 (4)					23.8	1664 (104)		67 (9654)
–2.0	14 (2)	41 (6)					23.8	1664 (104)	0.4	56 (8128)
–0.5	41 (6)	14 (2)	23	1669 (104)	0.10	31 (4513)	23.8	1664 (104)		19 (2767)
–0.5	28 (4)	14 (2)	23	1669 (104)	0.01	28 (3989)	23.8	1664 (104)		19 (2715)
–0.5	14 (2)	14 (2)					23.8	1664 (104)		18 (2625)
0.5	41 (6)	14 (2)	23	1669 (104)	0.17	15 (2200)	23.8	1664 (104)		14 (2056)
0.5	28 (4)	14 (2)	23	1669 (104)	0.17	14 (2039)	23.8	1664 (104)		13 (1945)
5.0	41 (6)	14 (2)	23	1669 (104)	0.29	16 (2328)	23.8	1664 (104)	0.4	12 (1793)
5.0	28 (4)	14 (2)	23	1669 (104)	0.22	15 (2140)	23.8	1664 (104)	0.4	12 (1701)

Table 11. Average resilient modulus of subgrade soils as a function of temperature.

°C	*NH5*	*NH4*	*NH2*	*NH3*	*NH1*
20.0			59 (8505)	289 (41,904)	45 (6570)
5.0	47 (6795)	35 (5080)	55 (7985)		43 (6284)
0.5	52 (7516)	38 (5458)	52 (7535)	315 (45,756)	54 (7820)
–0.5	40 (5846)	3569 (517,576)	299 (43,310)	349 (50,583)	497 (72,099)
–2.0	225 (32,653)	13,276 (1,925,517)	3585 (519,960)	1974 (286,245)	2736 (396,763)
–5.0	1143 (165,769)	17,556 (2,546,266)	6174 (895,404)	2424 (351,524)	9737 (1,412,232)
–10.0	2861 (414,959)	21,198 (3,074,546)	10,562 (1,531,915)	2527 (366,486)	15,833 (2,296394)
–20.0	5335 (773,768)				
–10.0	3106 (450,546)				14,818 (2,149,167)
–5.0	1586 (230,002)	18,064 (2,620,028)	6931 (1,005,290)	2452 (355,607)	7107 (1,030,833)
–2.0	106 (15,445)	12,434 (1,803,385)	3851 (558,608)	2017 (292,569)	3327 (482,500)
–0.5	24 (3477)	6386 (926,212)	577 (83,617)	995 (144,353)	1315 (190,736)
0.5	14 (2060)	15 (2108)	49 (7166)	223 (32,279)	176 (25,578)
5.0	14 (1991)	10 (1482)			
20.0			48 (6981)	220 (31,863)	38 (5451)

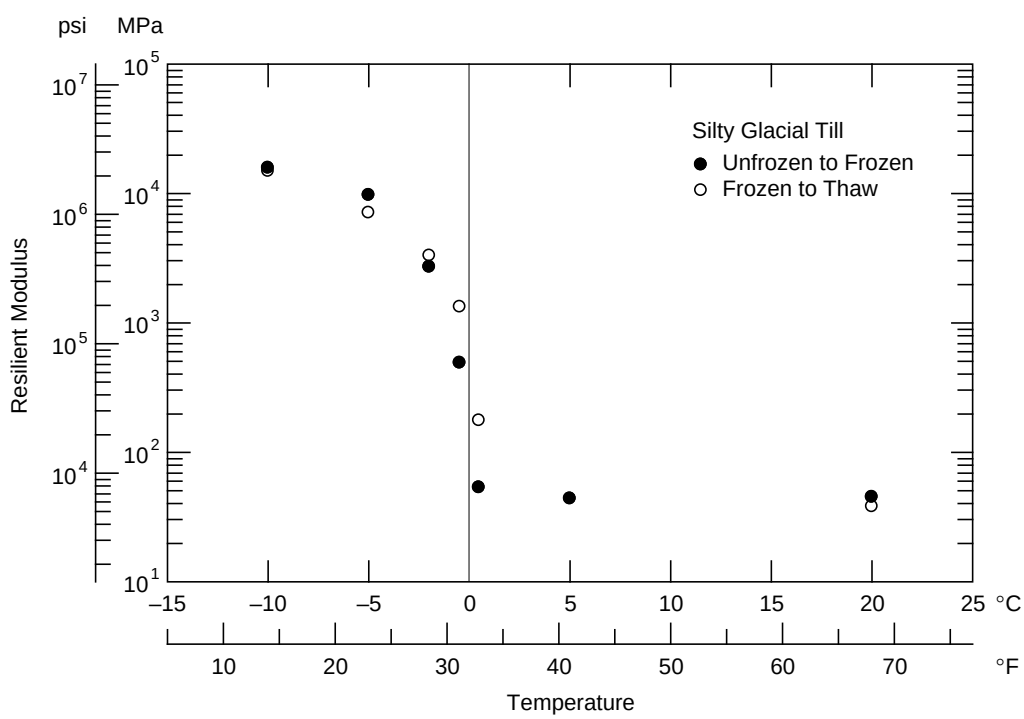

Figure 5. Effect of freezing and thawing on the resilient modulus of silty glacial till.

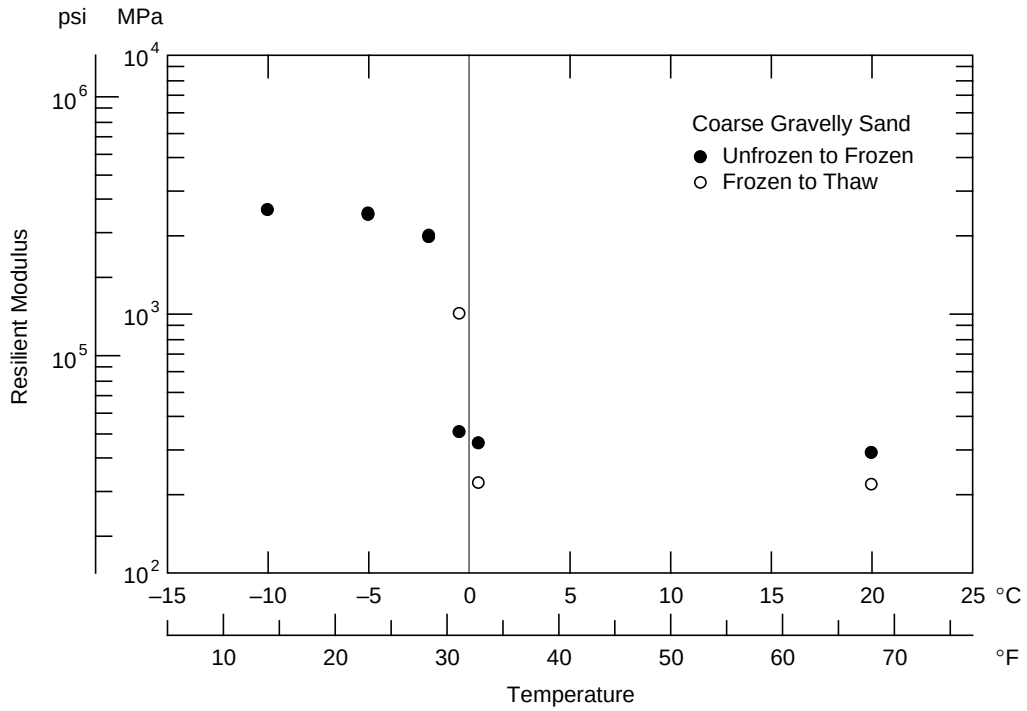

Figure 6. Effect of freezing and thawing on the resilient modulus of coarse gravelly sand.

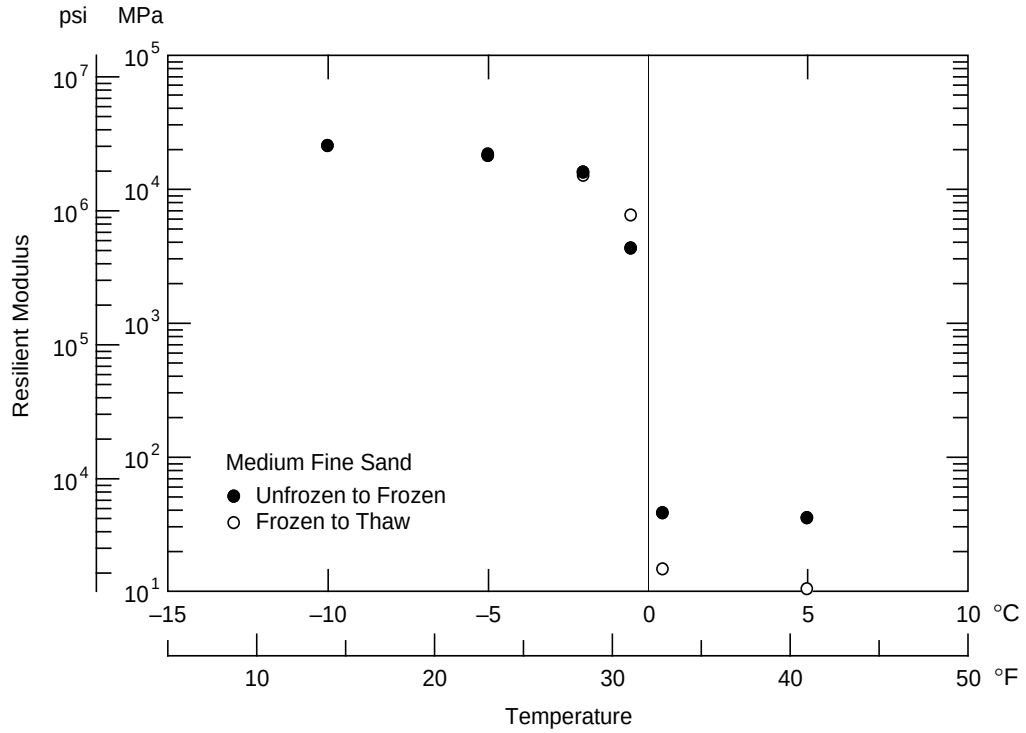

Figure 7. Effect of freezing and thawing on the resilient modulus of fine sand.

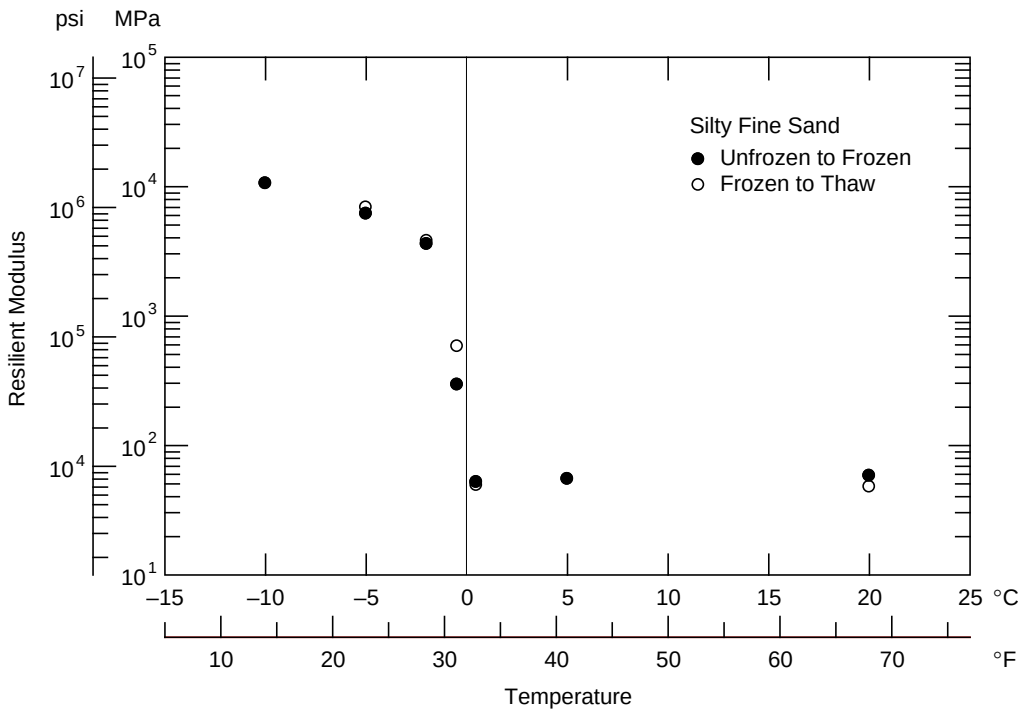

Figure 8. Effect of freezing and thawing on the resilient modulus of silty sand.

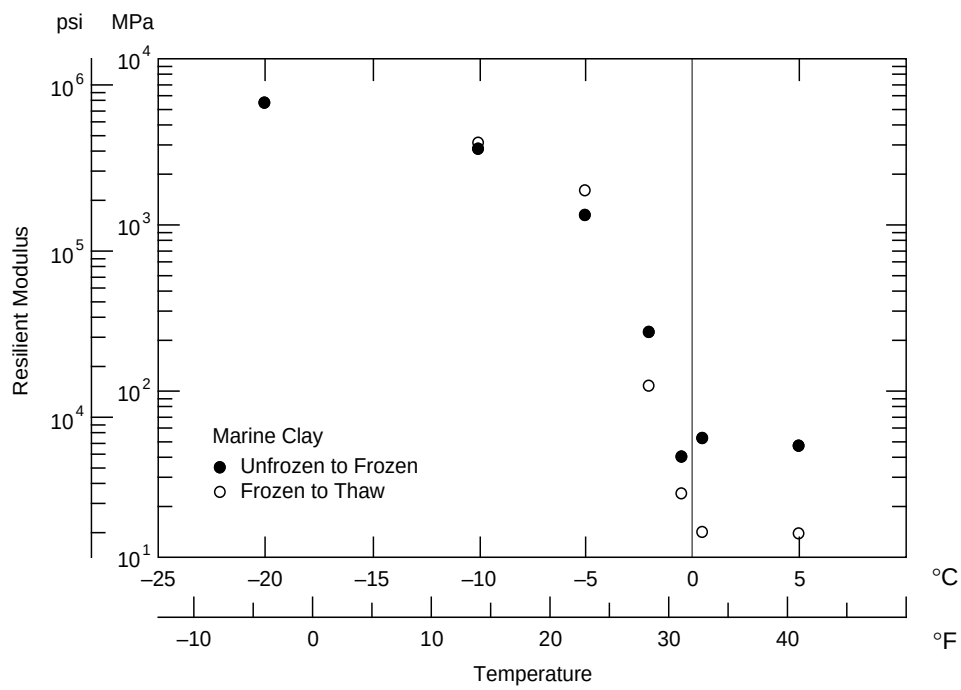

Figure 9. Effect of freezing and thawing on the resilient modulus of marine clay.

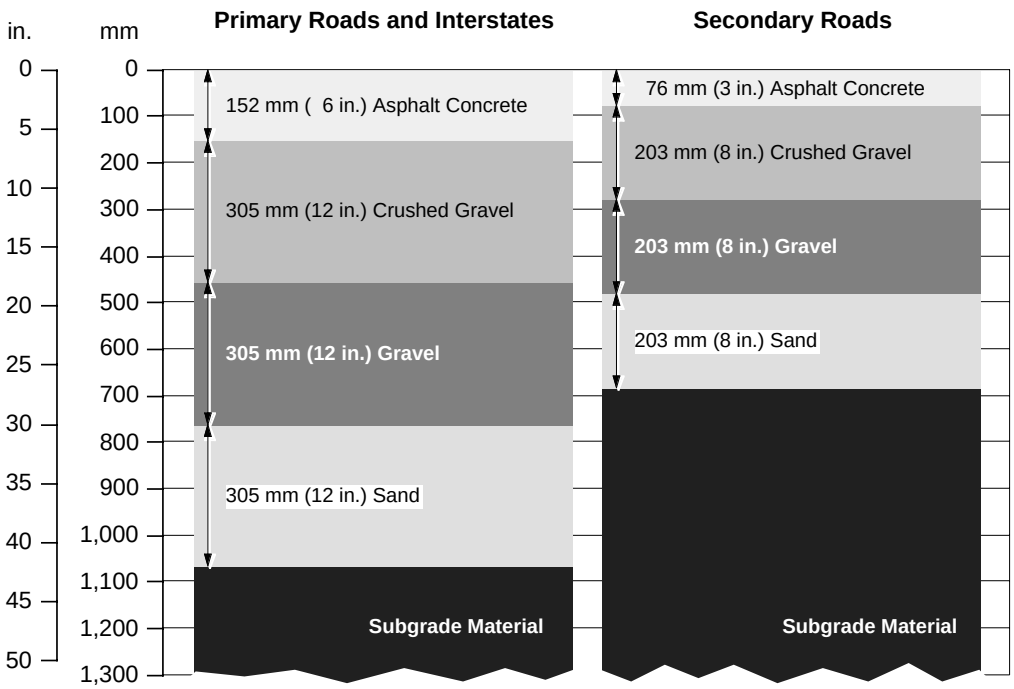

Figure 10. Typical pavement cross sections used by NHDOT.

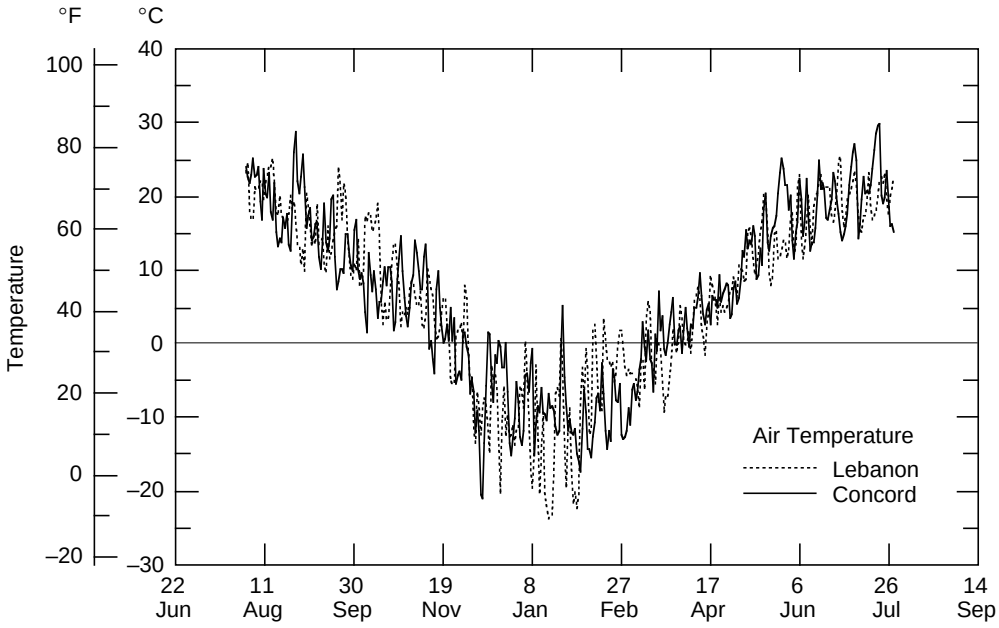

Figure 11. Design air temperatures used for estimating subgrade temperatures.

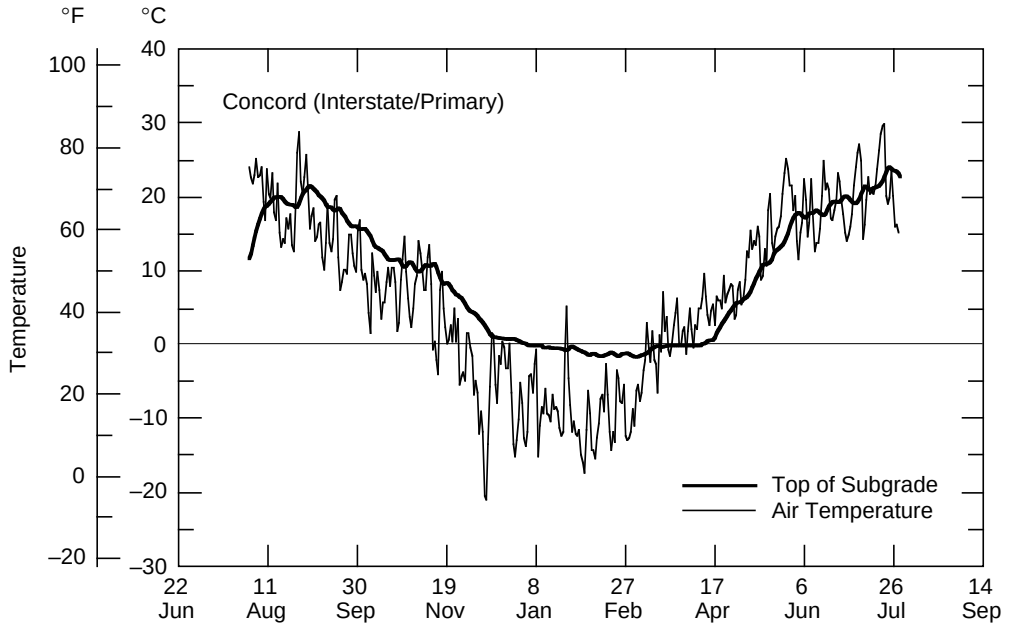

Figure 12. Annual temperature at the top of the subgrade (interstate pavement system), Concord, New Hampshire.

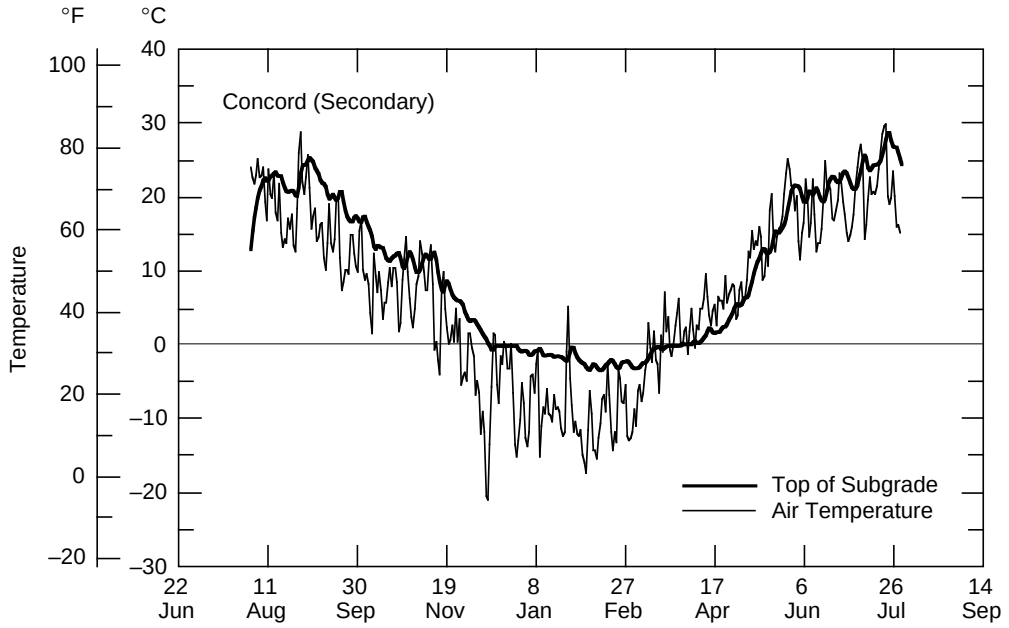

Figure 13. Annual temperature at the top of the subgrade (secondary pavement system), Concord, New Hampshire.

Table 12. Estimated mean top of the subgrade temperatures (°C) from FROST.

		Subgrade	
	Air	*Interstate*	*Rural*
January	–8.2	–0.2	–1.2
February	–10.4	–1.5	–3.0
March	–1.3	–0.5	–1.0
April	5.0	1.9	2.2
May	15.1	11.0	13.2
June	18.1	18.5	21.4
July	21.4	21.6	24.9
August	19.9	18.6	21.7
September	14.5	18.8	20.4
October	8.0	12.7	13.1
November	4.0	8.8	8.7
December	–6.5	2.0	0.7

Table 13. Temperatures for selecting subgrade modulus.

	Temperature (°C)	
Months	*Interstate*	*Secondary*
January	– 0.5	–1.5
February	–1.5	–3.0
March	–1.0 & 0.1	–3 & 0
April	0.5 & 4	0 & 3
May	11	13
June	18	21
July	22	25
August	19	22
September	19	20
October	13	13
November	9	9
December	2	2 & 0

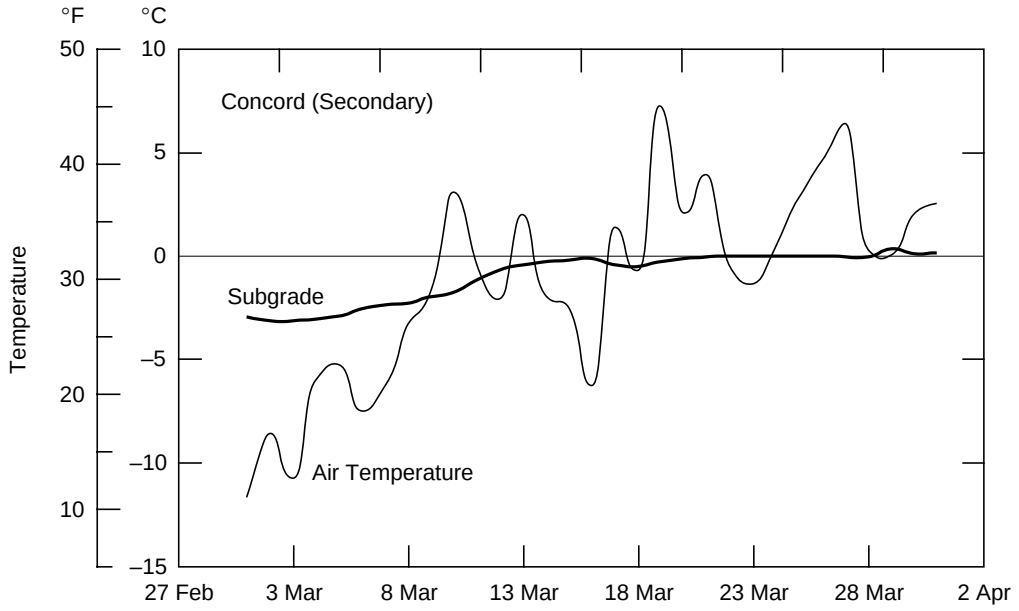

a. Secondary road at Concord, New Hampshire.

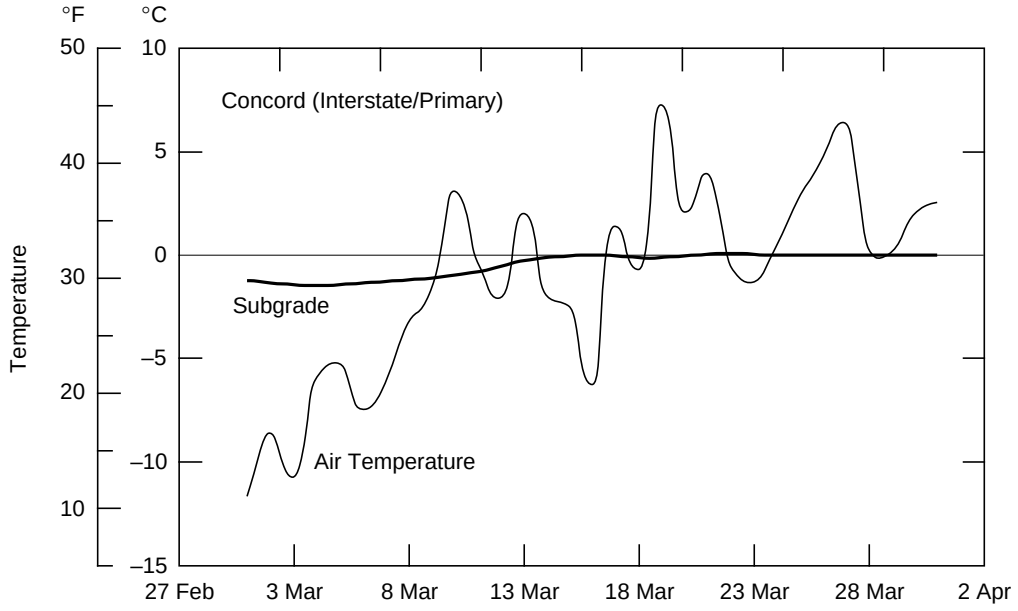

b. Primary (interstate) road at Concord.

Figure 14. Example of a rapid change of subgrade temperature during thawing.

Table 14a. Effective resilient modulus for NH5 for interstate and secondary pavements.

Interstate				*Secondary*			
Month	*Temp (°C)*	M_r, *MPa (psi)*	(u_f)	*Month*	*Temp (°C)*	M_r, *MPa (psi)*	(u_f)
January	–0.5	103 (15,000)	0.0242	January	–1.5	172 (25,000)	0.00739
February	–1.5	172 (25,000)	0.0001	February	–3	379 (55,000)	0.00001
March	–1	41 (6000)	0.0020	March	–3	379 (55,000)	0.00001
March	0.1	18 (2600)	1.4098	March	0	19 (2700)	1.29157
April	0.5	14 (2000)	2.5911	April	0	19 (2700)	1.29157
April	4	14 (2000)	2.5911	April	3	14 (2000)	2.59115
May	11	14 (2000)	2.5911	May	13	14 (2000)	2.59115
June	18	14 (2000)	2.5911	June	21	14 (2000)	2.59115
July	22	45 (6500)	0.1682	July	25	45 (6500)	0.16824
August	19	45 (6500)	0.1682	August	22	45 (6500)	0.16824
September	19	45 (6500)	0.1682	September	20	45 (6500)	0.16824
October	13	45 (6500)	0.1682	October	13	45 (6500)	0.16824
November	9	45 (6500)	0.1682	November	9	45 (6500)	0.16824
December	2	45 (6500)	0.1682	December	2	45 (6500)	0.16824
Summation			12.8101	December	0	69 (10,000)	0.06193
Average			1.0675	Summation			11.43536
				Average			0.95295
Effective M_r =		20 (2931)		Effective M_r =		21 (3078)	

Table 14b. Effective resilient modulus for NH4 for interstate and secondary pavements.

Interstate				*Secondary*			
Month	*Temp (°C)*	M_r, *MPa (psi)*	(u_f)	*Month*	*Temp (°C)*	M_r, *MPa (psi)*	(u_f)
January	–0.5	4137 (600,000)	0.0000	January	–1.5	8618 (1,250,000)	0.00000
February	–1.5	8618 (1,250,000)	0.0000	February	–3	13,790 (2,000,000)	0.00000
March	–1	5516 (800,000)	0.0000	March	–3	13,790 (2,000,000)	0.00000
March	0.1	14 (2000)	2.5911	March	0	345 (50,000)	0.00148
April	0.5	14 (2000)	2.5911	April	0	345 (50,000)	0.00148
April	4	14 (2000)	2.5911	April	3	345 (50,000)	0.00148
May	11	34 (5000)	0.3092	May	13	14 (2000)	2.59115
June	18	34 (5000)	0.3092	June	21	34 (5000)	0.30922
July	22	34 (5000)	0.3092	July	25	34 (5000)	0.30922
August	19	34 (5000)	0.3092	August	22	34 (5000)	0.30922
September	19	34 (5000)	0.3092	September	20	34 (5000)	0.30922
October	13	34 (5000)	0.3092	October	13	34 (5000)	0.30922
November	9	34 (5000)	0.3092	November	9	34 (5000)	0.30922
December	2	34 (5000)	0.3092	December	2	34 (5000)	0.30922
Summation			10.2472	December	0	345 (50,000)	0.00148
Average			0.8539	Summation			4.76163
				Average			0.39680
Effective M_r =		22 (3227)		Effective M_r =		31 (4490)	

Table 14c. Effective resilient modulus for NH2 for interstate and secondary pavements.

Interstate				*Secondary*			
Month	*Temp (°C)*	M_r, *MPa (psi)*	(u_f)	*Month*	*Temp (°C)*	M_r, *MPa (psi)*	(u_f)
January	–0.5	290 (42,000)	0.0022	January	–1.5	1379 (200,000)	0.00006
February	–1.5	1379 (200,000)	0.0001	February	–3	4137 (600,000)	0.00000
March	–1	689 (100,000)	0.0003	March	–3	4137 (600,000)	0.00000
March	0.1	124 (18,000)	0.0158	March	0	124 (18,000)	0.01584
April	0.5	124 (18,000)	0.0158	April	0	124 (18,000)	0.01584
April	4	55 (8000)	0.1039	April	3	55 (8000)	0.10392
May	11	55 (8000)	0.1039	May	13	55 (8000)	0.10392
June	18	55 (8000)	0.1039	June	21	55 (8000)	0.10392
July	22	55 (8000)	0.1039	July	25	55 (8000)	0.10392
August	19	55 (8000)	0.1039	August	22	55 (8000)	0.10392
September	19	55 (8000)	0.1039	September	20	55 (8000)	0.10392
October	13	55 (8000)	0.1039	October	13	55 (8000)	0.10392
November	9	55 (8000)	0.1039	November	9	55 (8000)	0.10392
December	2	55 (8000)	0.1039	December	2	55 (8000)	0.10392
Summation			0.9696	December	0	124 (18,000)	0.01584
Average			0.0808	Summation			0.98289
				Average			0.08191
Effective M_r =		61 (8917)		Effective M_r =		61 (8865)	

Table 14d. Effective resilient modulus for NH1 for interstate and secondary pavements.

Interstate				*Secondary*			
Month	*Temp (°C)*	M_r, *MPa (psi)*	(u_f)	*Month*	*Temp (°C)*	M_r, *MPa (psi)*	(u_f)
January	–0.5	483 (70,000)	0.0007	January	–1.5	1379 (200,000)	0.00006
February	–1.5	1379 (200,000)	0.0001	February	–3	4137 (600,000)	0.00000
March	–1	1379 (200,000)	0.0001	March	–3	4137 (600,000)	0.00000
March	0.1	55 (8000)	0.1039	March	0	172 (25,000)	0.00739
April	0.5	41 (6000)	0.2026	April	0	172 (25,000)	0.00739
April	4	41 (6000)	0.2026	April	3	41 (6000)	0.20257
May	11	41 (6000)	0.2026	May	13	41 (6000)	0.20257
June	18	41 (6000)	0.2026	June	21	41 (6000)	0.20257
July	22	41 (6000)	0.2026	July	25	41 (6000)	0.20257
August	19	41 (6000)	0.2026	August	22	41 (6000)	0.20257
September	19	41 (6000)	0.2026	September	20	41 (6000)	0.20257
October	13	41 (6000)	0.2026	October	13	41 (6000)	0.20257
November	9	41 (6000)	0.2026	November	9	41 (6000)	0.20257
December	2	41 (6000)	0.2026	December	2	41 (6000)	0.20257
Summation			2.1304	December	0	172 (25,000)	0.00739
Average			0.1775	Summation			1.84535
				Average			0.15378
Effective M_r =		44 (6351)		Effective M_r =		47 (6757)	

Table 15. Summary of effective resilient modulus for New Hampshire subgrade soils.

Soil type	Effective resilient modulus, MPa (psi)	
	Interstate/Primary	*Secondary*
Silt, some fine sand. Some coarse to fine gravel, trace coarse to medium sand (glacial till) – NH1	44 (6351)	47 (6757)
Fine sand, some silt – NH2	61 (8917)	61 (8865)
Coarse to fine gravelly, coarse to medium sand, trace fine sand – NH3	259 (37,535)	280 (40,678)
Coarse to medium sand, little fine sand – NH4	22 (3227)	31 (4490)
Clayey silt (marine deposit) – NH5	20 (2931)	21 (3078)

the tables are calculated using eq 4: and the effective resilient modulus (M_{eff}, psi) is calculated using eq 6:

$$M_{\text{eff}} = \left(\frac{u_{\text{f}}}{1.18 \times 10^{8}} \right)^{\frac{1}{2.32}} . \qquad (5)$$

RECOMMENDATIONS/CONCLUSIONS

This report describes the results of resilient modulus tests conducted on five subgrade soils commonly found in the state of New Hampshire. Based on the results from these tests, the effective resilient modulus was determined for use in design and evaluation of pavement structures. The effective resilient modulus of the subgrade soil under the interstate system was found to be similar to that of the secondary pavements. The recommended values are presented in Table 16.

It must be noted that these effective resilient moduli were obtained for soils at one moisture content and density, i.e., at the optimum density and moisture content. These values should be used with reservation at other densities and moisture contents. It is recommended that for general use within the state, additional tests be conducted to determine the effective resilient modulus as a function of moisture. It is also recommended that the remaining shear and hydrostatic compression tests be completed for prediction of pavement rutting during thaw periods.

Table 16. Recommended effective moduli for subgrade soils.

Subgrade type	Effective subgrade modulus, MPa (psi)
Silt, some fine sand. Some coarse to fine gravel, trace coarse to medium sand (glacial till) – NH1	45 (6500)
Fine sand, some silt – NH2	62 (9000)
Coarse to fine gravel, coarse to medium sand, trace fine sand – NH3	265 (38,500)
Coarse to medium sand, little fine sand – NH4	26 (3800)
Clayey silt (marine deposit) – NH5	21 (3000)

LITERATURE CITED

AASHTO (1996a) Guide for design of pavement structures. American Association of State Highway and Transportation Officials.

AASHTO (1996b) AASHTO provisional method for determining the resilient modulus of soils and aggregate materials. AASHTO Provisional Standard TP46-94, Edition 1A.

Baltzer, S., and L. Irwin (1995) Characterization of subgrade materials, specimen preparation and test plan for repeated load triaxial testing. Cornell University Report 95-7.

Highway Research Board (1962) The AASHO road test: Summary report. Report 7, National Academy of Sciences–National Research Council, Washington D.C., publication 1061.

Guymon, G.L., R.L. Berg, and T.V. Hromadka (1993) Mathematical model of frost heave and thaw settlement in pavements. CRREL Report 93-2.

Simonsen, E., V. Janoo, and U. Isacsson (in preparation) Resilient properties of unbound road materials during seasonal frost conditions.

APPENDIX A: UNIFORM DENSITY AND MOISTURE CONTENT

Before the fabrication of the test specimens, a small study was conducted to develop a method for preparing samples with a uniform density and moisture content using the kneading compactor. The focus was on uniform density, as uniform moisture contents were easily obtained by thoroughly mixing the soil with the right amount of water. The approach used was similar to that of Baltzer and Irwin (1995). They found through experimentation that by controlling the compaction load and number of tamps, they were able to produce uniform density A-4 test specimens within tolerable limits.

For the sands and the fine-grained soils, the test material was material finer then the no. 4 sieve. For the coarser A-1-a and the A-4 soils, aggregates larger than 1.5 in. (38 mm) were removed from the test gradation. The test sample dimensions for the sands and fine-grained soils was 2.8 in. (71 mm) in diameter and 6.0 in. (152 mm) tall. For the coarse-grained soils, the sample size was 6.0 in. (152 mm) in diameter and 12.0 in. (304 mm) high. These sizes are in accordance to the AASHTO Provisional Standard TP46-94.

The procedure developed was similar for both types of soils, with some exceptions. Test samples were compacted in specially designed cylinders of split ring developed for both the 2.8-in.- (71-mm-) and 6-in.- (152-mm-) diam. test specimens (Fig. A1). The rings for the fine-grained soils were made from aluminum and were 1 in. (25 mm) in height. For the coarse- and fine-grained soils, the rings were made from plastic and were 2 in. (50 mm) in height. These rings were stacked in an aluminum cylinder. For the fine-grained soils, the outer ring was made from plastic, whereas for the coarse-grained material it became necessary to make the outer ring (split mold) from aluminum (Fig. A2) because of the higher compaction pressures. The high pressures were causing the plastic outer ring to deform. The additional ring on top was used to compact an additional layer. We found in previous attempts that the density of the top layer was always lower than the remaining

Figure A1. Split ring mold used for uniform density verification tests.

Figure A2. Test apparatus for coarse-grained soils.

Figure A3. Apparatus in kneading compactor.

layers in the test specimen. The apparatus was placed in the kneading compactor and compacted in five layers at optimum density and moisture content (Fig. A3).

The kneading compactor was the CS 1200 electrohydraulic kneading compactor manufactured by James Cox & Sons, Inc. It was modified to make 2.8-in.- (71-mm-) and 6-in.- (152-mm-) diam. samples. Compaction was accomplished by applying a kneading pressure to the specimen through a tamping foot by means of a controlled dynamic force. The compactor has a rotating table and is electronically timed to the tamper foot. This kneading compactor can be programmed for pressure–time curves, repetition of rates, extended dwell times at peak pressure, and a variety of predetermined totals of compaction counts. The fine-grained material was compacted with a 3.15-in.^{2} (20.26-cm^2) tamper. The coarse-grained material was compacted with a 9.6-in.^{2} (62.06-cm^2) tamper.

At the end of sample compaction, the rings were extruded from the outer mold. For the 2.8-in. (71-mm) samples, a hand piston was used (Fig. A4). The additional layer was carefully removed prior to determining the density and moisture content in the remaining six layers (Fig. A5). The rings were removed one by one and the density and moisture content of each layer are determined (Fig A6). The same procedure was done for the coarse-grained soils. By this trial and error process, the required kneading pressures and tamps were developed for a uniform density and moisture content test specimen. Once the correct pressure and tamps were determined for each soil, the procedure was repeated five times to assure that the procedure produced repeatable results. For the marine clay, it was anticipated that test

Figure A4. Extrusion of rings for 71-mm samples.

Figure A5. Removal of top layer prior to density–moisture determination.

Figure A6. Removal of individual rings for density–moisture determination.

Table A1. Density–moisture results from compaction study.

AASHTO classifi-cation	*NHDOT classification*	*Dry density (kg/m³)*		*Moisture content (%)*		*COV as function of depth*
		Target	*Mean*	*Target*	*Mean*	*Density (%)*
A-2-4	Silty fine sand	1712	1661	14.5	13.8	1.4
A-7-5	Marine clay	1560	1514	21.0	22.5	0.9
A-7-5	Marine clay	1610	1633	23.5	23.3	0.9
A-7-5	Marine clay	1584	1582	25.0	25.5	1.1
A-4	Silty glacial till	2048	2115	9.0	10.4	0.8
A-1-b	Medium fine sand	1632	1640	13.6	14.3	1.2
A-1-a	Coarse gravely sand	1728	1840		2.4	

Table A2. Required number of tamps and kneading pressure to produce uniform density and moisture in test specimens.

						Kneading pressure	
Soil	*A-4*	*A-7-5*	*A-2-4*	*A-1-b*	*A-1-a*	*(psi)*	*(kPa)*
LAYER1	18	18	25*	15**	12	75	517
LAYER2	18	18	25**	15	12	75	517
LAYER3	12	12	25**	15	24	75	517
LAYER4	18	18	25**	15	24	75	517
LAYER5	24	24	25**	15	24	75	517

*Kneading pressure = 150 psi (1034 kPa).
**Kneading pressure = 125 psi (862 kPa).

specimens may be molded at several moisture contents. Therefore, compaction procedures were developed for three moisture contents. We were unable to split the coarse gravelly (A-1-a) material into the individual rings. The material had very little fines and there was no cohesion to hold the material in the individual rings. For this material, the density was determined from the total weight of the specimen. Table A1 shows the target and obtained dry densities, moisture contents, and the coefficient of variation of the densities and moisture contents.

To obtain uniform densities, the following number of tamps and kneading pressure were used as shown in Table A2. Layer 1 is at the bottom of the mold. Note that for the A-2-4 and the A-1-b soils, higher kneading pressures on the first layer were needed 150 and 125 psi (1034 and 862 kPa, respectively). For the remaining layers of A-2-4, the kneading pressure was decreased to 125 psi (862 kPa), with the same number of tamps used.

APPENDIX B: SAMPLE PREPARATION/TESTING

RESILIENT MODULUS TESTING

For resilient modulus test samples, the required amount of test material was soaked at the required moisture content for 24 hours. The samples were fabricated using the procedure in Appendix A.

A membrane is fitted around the bottom cap and securely fastened with two O-rings. The split aluminum mold (Fig. B1) is secured with two hose clamps, and the fasteners should be aligned so that the attaching rods to the bottom plate will pass freely. The membrane is then stretched over the top of the mold and securely fastened with an O-ring. For drained tests, a special porous plastic of higher porosity is used. Vacuum is applied through the side of the mold and the membrane is pulled tightly to the sidewalls.

The mold is transferred to the kneading compactor and fastened to the rotating base. The first layer of soil is added and tamped with the proper foot (depending on the diameter of the test specimen). The surface is scarified before the next layer is added. After the last layer has been placed and compacted, it is trimmed carefully and capped. The cap includes a filter paper and a top cap. The rubber membrane is placed over the top cap and then securely fastened with O-rings (Fig. B2).

For the fine-grained soils, the vacuum was released and the specimen transferred to either the MTS machine. For coarse-grained soil, for resilient modulus

Figure B1. Split aluminum mold for specimen preparation.

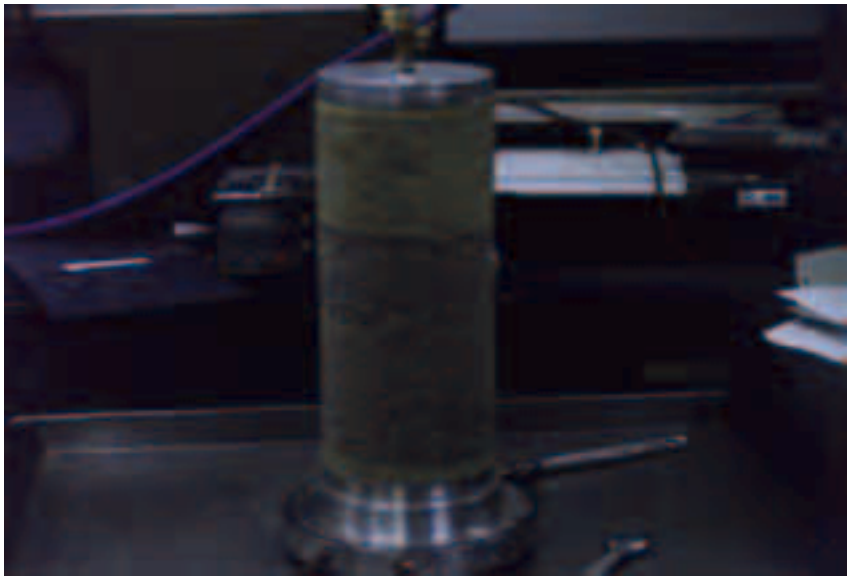

Figure B2. Specimen at the end of compaction.

tests below freezing, the specimens were frozen with a small vacuum on the sample. Once frozen, the vacuum was released. At above-freezing temperatures, the specimen was transferred to the MTS with a small vacuum on it.

The specimen was instrumented for measuring axial and radial deformations. The axial deformation in the middle third of the test specimen was monitored using two linear variable differential transformers (LVDTs). The middle third measurement position was chosen to reduce the effect of the nonuniform stresses at the boundary of the specimen and the end caps. The LVDTs are mounted on two spring-loaded circumferential rings on the specimen (Fig. B3). This is different from the

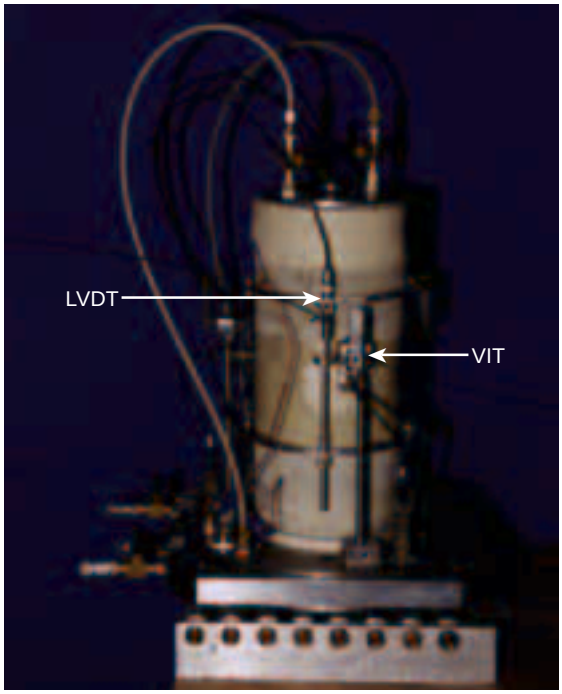

Figure B3. Instrumentation on test specimens showing LVDTs and multi-VITs.

AASHTO TP 46, where the LVDTs are placed on the outside of the chamber (Fig. B4). Deformation of the specimen is inferred from the movement of the loading piston rod. Our experience has shown that there can be significant differences between the measurements made from the piston rod and that made on the specimen. The difference has been attributed to friction as the rod slides through the cover plate. The LVDT barrels are mounted on the top ring and the tips of the spring loaded cores protrude to the bottom ring. An alignment jig was used during setup to ensure a uniform gage length for each test. The LVDTs have a range equal to or greater than 5% strain over the gauge length. The 2.8-in.- (71-mm-) diam., 6-in.- (152-mm-) tall specimens have a gauge length of 3 in. (75 mm) and the 6-in.- (152-mm-) diam. and 12-in.- (304-mm-) tall specimens have a gauge length of 6 in. (152 mm).

Radial displacements were measured with three noncontacting displacement transducers called multipurpose variable impedance transducers (multi-VITs) (Fig. B3). Brass targets were glued on to the specimens around the middle of the specimen. Each multi-VIT was calibrated with the aluminum foil targets and calibration curves of voltage vs. distance obtained. The multi-VITs are mounted on rods that bolt to the base of the triaxial cell. The position of each transducer is adjusted by a micrometer, which reacts against the spring loaded rod to which the transducer is attached. Early in the research, the three measurements are recorded and averaged from which the radial strain and Poisson's ratio are calculated. Later, we recorded each signal separately.

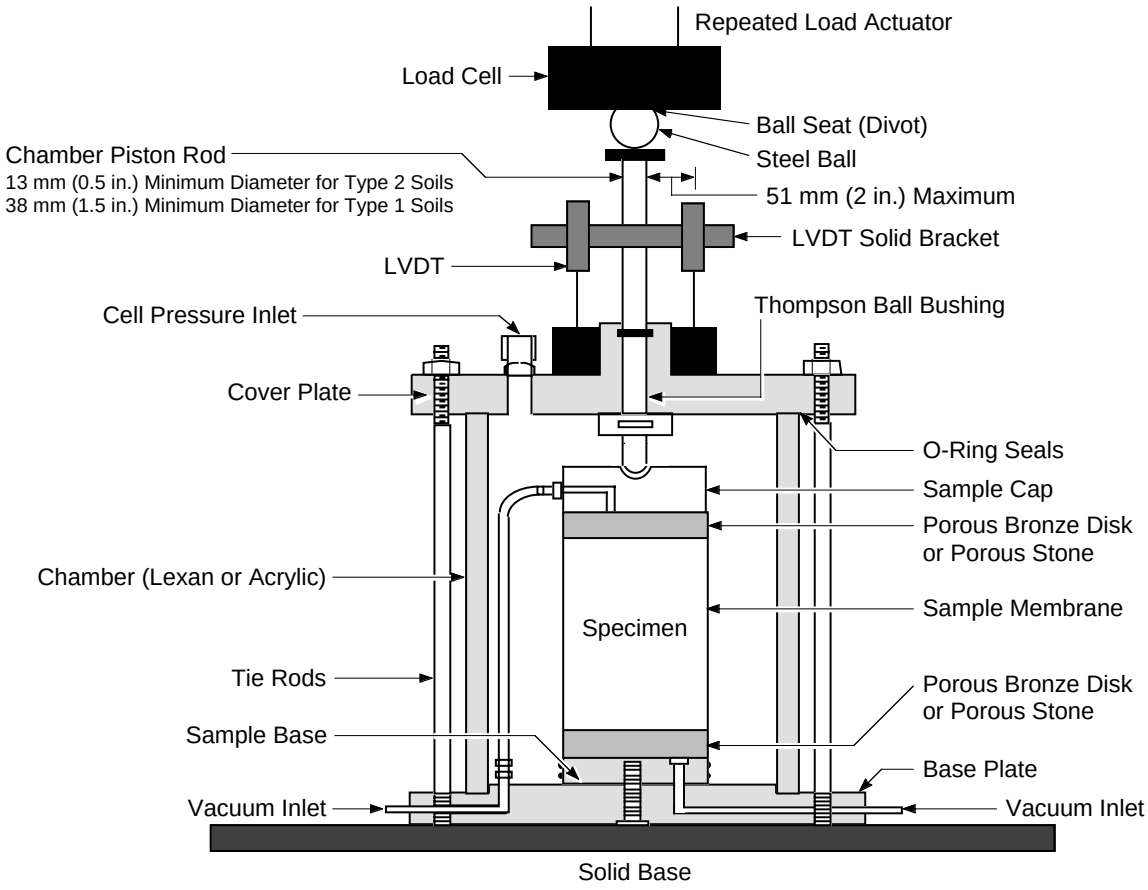

Figure B4. Typical AASHTO triaxial chamber with external LVDTs and load cell.

Figure B5. Complete test apparatus placed into environmental chamber.

After the instrumentation was completed, a Plexiglass cylinder with the multi-VIT micrometer heads through the wall was placed over the sample. The micrometer was used to set the range between the aluminum foil target and the transducer prior to testing. Threaded rods were then placed between the top and bottom cap and tightened to complete the assembly. The whole assembly was then moved into the environmental chamber, which is part of Figure B5.

Once in the MTS, a confining pressure is applied. The confining pressure applied was conditioning pressure suggested by AASHTO TP 46-94 and CRREL test protocol. For the cohesive soil, the specimen was cured for a minimum of three days before testing so as to reduce the effect of thixotropy. For the cohesionless soil, since thixotropy was not an issue, there was no curing time.

TEST METHOD

Testing was performed on a closed loop electrohydraulic testing machine. The resilient modulus tests were run under load control using the AASHTO TP46 test protocol. Load pulses of 0.1-second and 0.9-second rests as suggested by the test protocol were used. Depending on the soil type, AASHTO standard TP46, Tables 1 and 2, were followed closely for the nonfrozen and thawed loading sequence. At times, the complete sequence could not be attained because of large deformations in the soil samples. During the tests, the rate of deformation was continuously checked and the sequence stopped if the predicted rate at the end of the load cycle was ≥ 2%. For the frozen resilient modulus tests, the suggested AASHTO loading

sequences (Tables 1 and 2) produced very small deformations. It was difficult to distinguish the response of the test specimen from the noise in the system. A series of static confined compression tests were carried out to determine the deviator stress at which the specimen response was still linear and produced sufficient deformation.

During some of the frozen tests, some load sequences were increased so that a signal from the transducers could be obtained for recording. When shear tests were performed, they were conducted using a constant piston rate of 3.05 mm/minute in displacement control. The loading sequence used for the test program are shown in Tables 7 to 12. The seating load in all cases was set to 10% of the maximum axial load as done in AASHTO TP 46.

Confining pressure was applied to the test specimen via the in-house pressurized air system. A bleeder type regulator was used to obtain the desired pressure, and a pressure transducer was used to monitor the confining pressure through out the test. A miniature, high-precision load cell mounted inside the triaxial cell on the loading piston was used to monitor the load applied to the specimen. The specimens were preconditioned with 500 load repetitions.

National Instruments Labview data acquisition software was used to collect the raw data. For the resilient modulus tests, each load sequence contained 100 cycles as long as the permanent displacement was within 5%. The last five cycles were recorded and stored for analysis. Data were acquired at 500 Hz. For the shear tests and hydrostatic compression tests, data were acquired at 5 Hz. The resilient modulus was determined by the method described in AASHTO TP46.

REPORT DOCUMENTATION PAGE

Form Approved
OMB No. 0704-0188

1. AGENCY USE ONLY (Leave blank)

2. REPORT DATE
September 1999

3. REPORT TYPE AND DATES COVERED

4. TITLE AND SUBTITLE
Resilient Modulus for New Hampshire Subgrade Soils for Use in Mechanistic AASHTO Design

5. FUNDING NUMBERS
Project: 12323P

6. AUTHORS
Vincent C. Janoo, Jack J. Bayer Jr., Glenn D. Durell, and Charles E. Smith Jr.

7. PERFORMING ORGANIZATION NAME(S) AND ADDRESS(ES)
U.S. Army Cold Regions Research and Engineering Laboratory
72 Lyme Road
Hanover, New Hampshire 03755-1290

8. PERFORMING ORGANIZATION REPORT NUMBER
Special Report 99-14

9. SPONSORING/MONITORING AGENCY NAME(S) AND ADDRESS(ES)
State of New Hampshire
Department of Transportation
Concord, New Hampshire 03302

10. SPONSORING/MONITORING AGENCY REPORT NUMBER

11. SUPPLEMENTARY NOTES

12a. DISTRIBUTION/AVAILABILITY STATEMENT
Approved for public release; distribution is unlimited.
Available from NTIS, Springfield, Virginia 22161

12b. DISTRIBUTION CODE

13. ABSTRACT (*Maximum 200 words*)
Resilient modulus tests were conducted on five subgrade soils commonly found in the state of New Hampshire. Tests were conducted on samples prepared at optimum density and moisture content. To determine the effective resilient modulus of the various soils for design purposes, tests were conducted at room temperature and at freezing temperatures. The AASHTO TP 46 test protocol was used for testing room temperature and thawing soils. At freezing temperatures, the CRREL test protocol was used. The results from this test program are presented in this report. In addition, suggested effective resilient modulus for the five soils are presented.

14. SUBJECT TERMS
Cohesive soils
Effective resilient modulus
Freezing
Granular soils
Resilient modulus
Sample preparation
Thawing

15. NUMBER OF PAGES
43

16. PRICE CODE

17. SECURITY CLASSIFICATION OF REPORT	18. SECURITY CLASSIFICATION OF THIS PAGE	19. SECURITY CLASSIFICATION OF ABSTRACT	20. LIMITATION OF ABSTRACT
UNCLASSIFIED	UNCLASSIFIED	UNCLASSIFIED	UL